Hearing Research 413 (2022) 108254

Contents lists available at ScienceDirect

Hearing Research

journal homepage: www.elsevier.com/locate/heares

The intravenous administration of skin-derived mesenchymal stem cells ameliorates hearing loss and preserves cochlear hair cells in cisplatin-injected mice
SMSCs ameliorate hearing loss and preserve outer hair cells in mice

Stella Chin-Shaw Tsai[a,#], Frank Cheau-Feng Lin[b,#], Kuang-Hsi Chang[c,d,e], Min-Chih Li[f], Ruey-Hwang Chou[d,g,h], Mei-Yue Huang[i], Yen-Chung Chen[i], Chien-Yu Kao[j], Ching-Chang Cheng[k], Hung-Ching Lin[l,m], Yi-Chao Hsu[f,l,*]

[a] Department of Otolaryngology, Tungs' Taichung Metroharbor Hospital, Taichung, Taiwan
[b] School of Medicine, Chung Shan Medical University, Taichung, Taiwan
[c] Department of Medical Research, Tungs' Taichung Metroharbor Hospital, Taichung, Taiwan
[d] Graduate Institute of Biomedical Sciences, China Medical University, Taichung, Taiwan
[e] General Education Center, Jen-Teh Junior College of Medicine, Nursing and Management, Miaoli, Taiwan
[f] Institute of Biomedical Sciences, Mackay Medical College, New Taipei City, Taiwan
[g] Center for Molecular Medicine, China Medical University Hospital, Taichung, Taiwan
[h] Department of Biotechnology, Asia University, Taichung, Taiwan
[i] Maria Von Med-Biotechnology Co. Ltd., Taipei, Taiwan
[j] Medical and Pharmaceutical Industry Technology and Development Center, Taipei, Taiwan
[k] Laboratory Animal Service Center, Office of Research and Development, China Medical University, Taiwan
[l] Department of Audiology and Speech-Language Pathology, Mackay Medical College, New Taipei City, Taiwan
[m] Department of Otolaryngology, Mackay Memorial Hospital, Taipei, Taiwan

ARTICLE INFO

Article history:
Received 30 March 2020
Revised 12 March 2021
Accepted 13 April 2021
Available online 5 May 2021

Keywords:
Skin-derived mesenchymal stem cells
Cisplatin
Hair cells
Inner ear
Ototoxicity
Cell therapy

ABSTRACT

Mesenchymal stem cells (MSCs) can be isolated from different tissue origins, such as the bone marrow, the placenta, the umbilical cord, adipose tissues, and skin tissues. MSCs can secrete anti-inflammatory molecules and growth factors for tissue repair and remodeling. However, the ability of skin-derived MSCs (SMSCs) to repair cochlear damage and ameliorate hearing loss remains unclear. Cisplatin is a commonly used chemotherapeutic agent that has the side effect of ototoxicity due to inflammation and oxidative stress. This study investigated the effects of SMSCs on cisplatin-induced hearing loss in mice. Two independent experiments were designed for modeling cisplatin-induced hearing loss in mice, one for chronic toxicity (4 mg/kg intraperitoneal [IP] injection once per day for 5 consecutive days) and the other for acute toxicity (25 mg/kg IP injection once on day one). Three days after cisplatin injection, 1×10^6 or 3×10^6 SMSCs were injected through the tail vein. Data on auditory brain responses suggested that SMSCs could significantly reduce the hearing threshold of cisplatin-injected mice. Furthermore, immunohistochemical staining data suggested that SMSCs could significantly ameliorate the loss of cochlear hair cells, TUNEL-positive cells and cleaved caspase 3-positive cells in cisplatin-injected mice. Neuropathological gene analyses revealed that SMSCs treatment could downregulate the expression of cochlear genes involved in apoptosis, autophagy, chromatin modification, disease association, matrix remodeling, oxidative stress, tissue integrity, transcription, and splicing and unfolded protein responses. Additionally, SMSCs treatment could upregulate the expression of cochlear genes affecting the axon and dendrite structures, cytokines, trophic factors, the neuronal skeleton and those involved in carbohydrate metabolism, growth factor signaling, myelination, neural connectivity, neural transmitter release, neural transmitter response

* **Corresponding author at:** Institute of Biomedical Sciences Mackay Medical College No. 46, Sec. 3, Zhongzheng Rd., Sanzhi Dist., New Taipei City 252, Taiwan.
E-mail address: hsuyc@mmc.edu.tw (Y.-C. Hsu).
# These authors contributed equally.

https://doi.org/10.1016/j.heares.2021.108254

and reuptake, neural transmitter synthesis and storage, and vesicle trafficking. Results from TUNEL and caspase 3 staining further confirmed that cisplatin-induced apoptosis in cochlear tissues of cisplatin-injected mice could be reduced by SMSCs treatment. In conclusion, the evidence of the effects of SMSCs in favor of ameliorating ototoxicity-induced hearing loss suggests a potential clinical application.

1. Introduction

Millions of people worldwide experience hearing loss, predominantly sensorineural hearing loss (SHL) due to damage to or loss of sensory hair cells (HCs) (Almeida-Branco et al., 2015). Cochlear HCs are responsible for converting sound vibrations into electrical signals, which are subsequently transmitted through spiral ganglion neurons (SGNs) to the brain. Accumulating evidence suggests that mammalian HCs and SGNs cannot self-regenerate (Almeida-Branco et al., 2015). Once subject to stress or damage, these HCs and SGNs decline in number in the cochlea, resulting in SHL (Almeida-Branco et al., 2015). In the cochlea, outer hair cells (OHCs) are more sensitive than inner hair cells (IHCs) to damages caused by environmental stress, ototoxicity, and aging (Chen et al., 2003; Fan et al., 2019; Kecskemeti et al., 2019). Currently, only preventive approaches have been developed for SHL, and no approved chemical or biological drugs are available for its treatment (Fan et al., 2019).

Cisplatin is a chemotherapeutic drug used to treat many types of solid tumors, such as lung, head and neck, ovarian, bladder, testicular, and uterine cancers (Jamieson and Lippard, 1999; Vecerić-Haler et al., 2017). However, it tends to result in nephrotoxicity and ototoxicity (Ringborg, 1983). Ototoxicity of cisplatin occurs as a result of the depletion of antioxidant substances and an increase in lipid peroxidation, with resulting apoptotic damage to the OHCs and SGNs (Meng et al., 2018; Wang et al., 2016; Yang et al., 2018).

Mesenchymal stem cells (MSCs) are multipotent stem cells that can be isolated from a variety of tissues, primarily the bone marrow (BM) (Nicolay et al., 2016). The characteristics of MSCs include adherence to plastic in a culture and the capability of multipotential differentiation into osteoblasts, adipocytes, and chondrocytes (Kang et al., 2010). The skin has long been regarded as a potential source of tissue for regenerative medicine. Several studies have demonstrated that skin-derived mesenchymal stem cells (SMSCs) are capable of differentiating into neural-like cells for peripheral nerve regeneration (Park et al., 2012), alleviating atherosclerosis via modulating the activity of macrophage (Li et al., 2015a), and restoring premature ovarian failure in mice (Lai et al., 2014).

In this study, we characterized the properties of SMSCs and investigated their potential beneficial effects on cisplatin-induced ototoxicity.

2. Materials and methods

2.1. Isolation and characterization of SMSCs

SMSCs (AGERACELL) were prepared and provided by Maria Von Med-Biotechnology Co., Ltd,Taiwan. In brief, a sample of skin tissue (1–2 mm^2) was obtained from the pinna. Subsequently, SMSCs were primarily cultured from the skin tissue and were maintained in Dulbecco's modified Eagle's medium (DMEM; Gibco; Thermo Fisher Scientific, Inc., Waltham, MA, USA) containing 5% human platelet lysate (EMD Millipore Corporation, Billerica, MA, USA) and 1% sodium pyruvate (Thermo Fisher Scientific) at 37°C in 5% CO_2 in humidified air. After SMSCs were isolated, they were washed and maintained in DMEM containing 5% human platelet lysate. Cells were passaged every 4–6 days. All procedures and materials were modified from previous reports (Toma et al., 2001; Toma et al., 2005). MSC neurogenic differentiation medium (C-28015, PromoCell, Germany) containing 10 μM Y27632 (Sigma) was used to induce the neuronal differentiation of SMSCs, which were seeded at 4×10^3 cells/cm^2 on 6-well tissue culture plates coated with 10 μg/mL human fibronectin (Thermo Fisher Scientific). For the differentiation of SMSCs into adipocytes, osteoblasts, and chondrocytes, we followed the method and procedure reported by Li et al. (Li et al., 2013). In brief, for adipogenesis and osteogenesis differentiation, 3.8×10^4 and 1.9×10^4 SMSCs, respectively, were seeded in 24-well plates and grown for 3 days. Adipogenic and osteogenic differentiation media were replaced with fresh media every 3 days for 3 weeks. Adipocyte lipid droplets were stained with Oil Red O, and calcified osteoblasts were stained with Alizarin Red S. For chondrogenesis differentiation, 1×10^6 cells were placed in a 15-mL conical tube and centrifuged to form a pellet. Media were replaced with fresh media every 3 days for 3 weeks. Pellets were fixed in formalin and were sectioned. Chondrocytes were stained with Alcian blue. The generation and maintenance of human induced pluripotent stem cells (iPSCs) were processed according to our previous publication (Chen et al., 2018). We used the PSC neural induction medium (Thermo Fisher Scientific) to differentiate the neural progenitor cells (NPCs) from human iPSCs. Briefly, human iPSCs were seeded in the PSC neural induction medium. The medium was changed every day. Following the protocol provided in the manual instruction, we can obtain the iPSC-derived neural precursor cells (iPSC-derived NPCs) on Day 7 (P1). After two more passages, the iPSCs-derived NPCs (P3) were sent for whole transcriptome analysis by RNA sequencing technology.

2.2. Flow cytometry

SMSCs (1×10^6) were suspended in 100 μL of wash buffer consisting of phosphate-buffered saline (PBS) containing 0.5% bovine serum albumin and were labeled with phycoerythrin (PE) rat anti-mouse CD73 (1:100), PE rat anti-mouse CD90 (1:100), PE rat anti-mouse CD105 (1:100), and a PE human mesenchymal stem cell lineage antibody cocktail (containing CD34, CD45, CD11b, CD19, and HLA-DR) (1:100). Antibodies were added to each of the tubes and incubated at room temperature for 30 minutes. Cells were then washed three times and suspended in PBS for flow cytometry analysis. PE-conjugated isotype antibodies were used to characterize nonspecific staining. Cells were analyzed using a CytoFLEX flow cytometer (Beckman Coulter, Brea, CA), and data were analyzed using FlowJo software.

2.3. Transplantation of SMSCs, total body weight assessment, tissue preparation, and mating trials

The Animal Care Committee of Mackay Medical College approved the animal experiments in this study. C57BL/6 female mice (8 weeks old) were purchased from BioLasco (Taiwan). All animals were bred and housed in accordance with the standard animal protocol. For the cisplatin chronic or acute toxicity experiment, cisplatin was dissolved in 0.1% dimethyl sulfoxide to induce ototoxicity in mice through intraperitoneal (IP) injection; procedures were implemented in accordance with the protocol reported by Wu et al. (Wu et al., 2017). The treatment group received 100 μL of serum-free DMEM containing 3×10^6 (n = 6) SMSCs,

and the control group received only DMEM (100 μL; n = 6). For the experimental group, 100 μL of serum-free DMEM containing 1×10^6 (n = 9) SMSCs, the DMEM containing 3×10^6 (n = 9) SMSCs, or 100 μL of medium (n = 9, as the untreated control group) was systemically administered through injection into the tail vein 3 days after cisplatin injection. After SMSC injection, the body weight of mice in all groups was measured. All mice underwent auditory brainstem response (ABR) measurements under anesthesia. Cochlear tissues were collected for further gene expression analyses.

2.4. Whole transcriptome analyses for SMSCs

Total RNA was isolated and used as the template for library construction according to the method detailed in our previous study (Chen et al., 2018). Genomics, Inc., Taiwan performed the total RNA sequencing (RNA-seq) and bioinformatics analyses. The importance of the relative abundance of each gene's expression level was analyzed according to the real fold change among the groups. Posterior probability of equal expression (PPEE) was used to evaluate the significance of differentially expressed genes. A significant expression difference was PPEE< 0.05.

2.5. NanoString gene expression analysis

Total mRNA was extracted from mouse cochlear tissues in each group. Genes involved in neuropathological processes were analyzed using a NanoString mouse neuropathology panel (NanoString Technologies Inc., Seattle, WA, USA). Gene expression values are presented as a percentage of the control group. Cold Spring Biotech, Corp., in Taiwan performed NanoString gene expression analysis and bioinformatics analyses. The NanoString neuropathological gene expression panel includes genes involved in many biological pathways and cell types (Rubino et al., 2018; Spangenberg et al., 2019). The results of a pathway score or cell type-specific score analyses can be complementary to those obtained from one more focused on individual genes. A web program PLAGE (Pathway Level Analysis of Gene Expression) for performing the kinds of analyses described in the literature (Tomfohr et al., 2005). Gene or pathway scores are used to summarize the data from a pathway's or cell type-specific genes into a single score by using nCounter® Advanced Analysis Software (version 2.0.134; https://www.nanostring.com/products/analysis-software/advanced-analysis). These scores are calculated as the first principal component of the pathway genes' normalized expression. All the analyses of gene or pathways scores were according to the user manual of nCounter® Advanced Analysis Software.

2.6. Whole-mount dissection, confocal microscopy, and the loss of OHC count

Experimental mice were anesthetized, and their cochlear tissues were isolated and dissected. For whole-mount dissection, we followed the protocol detailed by Neal et al. (Neal et al., 2015). In brief, the cochlea was decalcified for 1 hour using a decalcification solution purchased from Apex Engineering (Aurora, IL, USA). The excess temporal bone around the cochlea was trimmed, and the cochlea was bisected along the midmodiolar plane and then submerged in PBS. A series of cuts through the modiolus separated the half-turns from one another. Each half-turn was then removed from the surrounding temporal bone, and the tectorial membrane was removed. The cochlear tissues were fixed with 4% paraformaldehyde. The tissues were incubated with the primary antibodies of anti-Myo7a (1:100, Santa Cruz, CA) and anti-phalloidin conjugated with Alexa 488 (1:200, Thermo Fisher Scientific) at 4°C overnight and at 4°C for 2 h, respectively. The tissues were incubated with the secondary antibody of rhodamine goat antimouse (1:200, KPL) at room temperature for 2 h. Cells were stained with DAPI (Sigma). For the loss of OHCs counts, HCs were counterstained with phalloidin, Myo7a and DAPI stainings. Images were captured using a confocal spectral microscope (Leica SP8). We acquired images at three randomly-selected regions (300 μm length) in the apical, middle, and basal cochlear turns by using the same apparatus, and manually counted the loss of OHCs. Average loss of OHCs were then calculated in apex, middle and base regions, respectively (Ninoyu et al., 2020).

For the TUNEL (Terminal deoxynucleotidyl transferase-mediated dUTP nick-end labeling) assay. TUNEL staining was performed in the cochlear tissues according to the manufacturer's instructions (Vazyme, A112). In addition, the cochlear tissues were fixed with 4% paraformaldehyde. The primary antibodies, anti-cleaved caspase-3 (1:200; Cell Signaling Technology) was incubated at 4°C overnight. The secondary antibodies, Rhodamine goat-anti-Rabbit (1:200, KPL) were incubated at room temperature for 2 h. Cells were stained with DAPI (Sigma). Fluorescent images were taken with a Leica SP8 confocal fluorescence microscope.

2.7. ABR measurement

In the present study, we measured the ABR of mice to detect their hearing threshold. In brief, measurements were performed on the scalps of mice under anesthesia by using subdermal needle electrodes placed at the vertex, below the pinna of the left ear (as a reference measurement), and below the contralateral ear (ground). The sound stimuli included clicks (100-ms duration; 4, 8, and 12 kHz). The devices used for ABR measurement in this study were specifically designed for animal experiments (BIOPAC System, USA). Acoustic stimuli were applied directly to the ear canal at a stimulus intensity ranging from a 100-dB to a threshold 10-dB sound pressure level at 10-dB intervals near the threshold level. The ABR threshold was measured through detection of the presence of V waves. All procedures for ABR measurement were modified from previous reports (Akil et al., 2016; Choi et al., 2012; Ingham et al., 2011).

2.8. Statistical analyses

Data are expressed as inter quartitle range (IQR) and median. Nonparametric statistical tests (Kruskal–Wallis and Mann–Whitney U tests) were performed using SPSS 17.0 software. Bonferroni correction was used for multiple analysis. Statistical significance was defined as $P < 0.005$ in Fig. 3 and $P < 0.008$ in Figs. 4, respectively.

3. Results

3.1. Preparation and characteristics of SMSCs

After primary culture of SMSCs, SMSCs were frozen in liquid nitrogen. Flow cytometry was then applied to examine the characteristics of MSCs, including specific cell surface markers and differentiation capacity, and the results were obtained as follows: 99.6% CD73(+), 99.3% CD90(+), and 98.8% CD105(+). Furthermore, CD34, CD45, and CD11b expression was not detected in SMSCs (Fig. 1A). Additionally, SMSCs could be differentiated into adipocytes, osteoblasts, and chondrocytes (Fig. 1B), indicating a differentiation capacity for cells of mesenchymal origins similar to those of MSCs. During development, skin tissues form first in the ectoderm. We thus examined the neural differentiation capacity of SMSCs and demonstrated that they could be further differentiated into NeuN(+) and MAP2(+) neurons (Fig. 1C), indicating the differentiation capacity of SMSCs into ectodermal neuronal lineages.

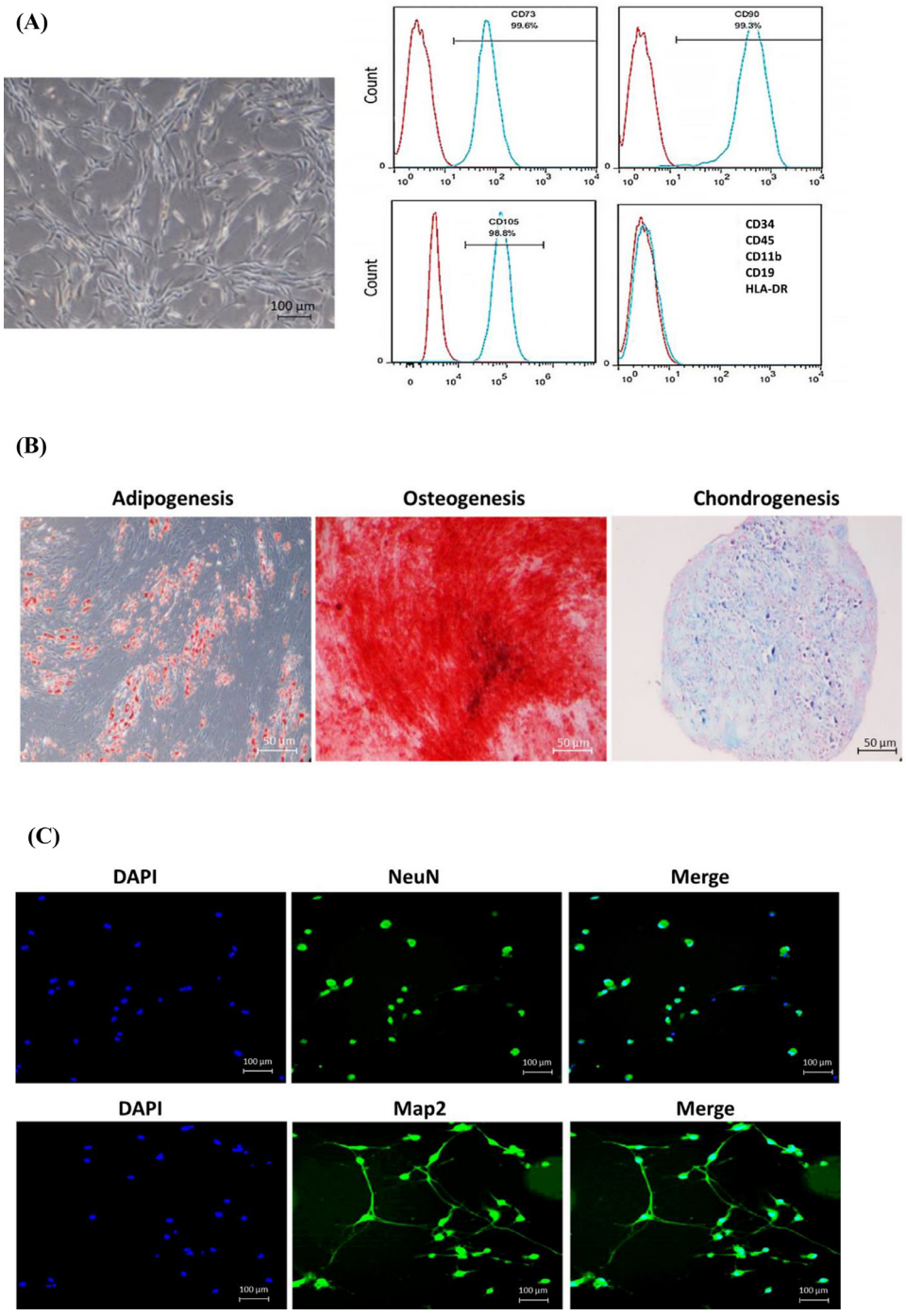

Fig. 1. Isolation and characterization of human skin-derived mesenchymal stem cells (SMSCs). (A) Human SMSCs have morphology similar to that of fibroblast cells, and analyses of the cell surface markers showed that SMSCs were CD73(+), CD90(+), and CD105(+), indicating that they expressed the definitive markers of MSCs. Scale bar = 100 μm. (B) The multipotent differentiation capacity of SMSCs was demonstrated for osteogenesis, adipogenesis, and chondrogenesis. Alizarin Red, Oil Red O, and Alcian Blue stainings were used to characterize osteoblasts, adipocytes, and chondrocytes, respectively. Scale bar = 50 μm. (C) The neuronal differentiation capacity of SMSCs was demonstrated for NeuN(+) and MAP2(+) neurons. Scale bar = 100 μm.

3.2. Whole transcriptome analyses of SMSCs

To examine the properties of SMSCs, we used RNA-seq technology to analyze the transcriptome of SMSCs. A real fold change comparison of the transcriptome of SMSCs with that of iPSC-derived NPCs after RNA-seq analyses revealed the top 20 upregulated and downregulated gene transcripts (Tables 1 and 2), upregulated stem cell marker and growth factor–related gene transcripts (Table 3), and downregulated stem cell marker and growth factor–related gene transcripts (Table 4) of SMSCs. The real fold change data of SMSCs and iPSC-derived NPCs revealed that compared with iPSC-derived NPCs, SMSCs had a higher expression level of mRNA encoding *SOX15* gene (Table 3) and higher expression levels of mRNAs encoding *PAX8*, *WNT5A*, *WNT5B*, *WNT11*, *VEGFB*, *PDGFD*, *FGF1*, *FGF5*, *FGF7* and *NGF* genes (Table 3). Additionally, SMSCs had lower expression levels of mRNAs encoding *SOX1*, *SOX2*, *SOX3*, *SOX5*, *SOX6*, *SOX10*, *SOX11*, *SOX13*, *SOX21*, *PAX2*, *PAX3*, *PAX6*, *PAX7*, and *IGF2* genes (Table 4). Supplementary Fig. 1 provides fur-

Table 1
Top 20 up-regulated genes in SMSCs versus iPSC-derived NPCs (iNPCs).

Top 20 up-regulated genes (SMSCs v. iNPCs)		
Gene Symbol	**Real Fold Changes**	**PPEE**
WISP2	1541476.609	1.11022E-16
ACKR4	936505.7028	2.22045E-15
NBL1	802878.6809	4.996E-15
DPT	473703.5398	7.67164E-14
CEMIP	6781.037087	1.66533E-14
NUPR1	6589.852647	1.92069E-14
NFIX	8060.83347	6.37268E-14
ANPEP	4218.259928	1.78746E-14
PSG5	354611.1265	3.4206E-13
PODN	5008.235917	7.93809E-14
ITGBL1	254304.4687	1.89981E-12
AKR1C3	4891.185613	7.31082E-13
MEG3	4579.419744	1.18117E-12
ANGPTL4	3358.434527	6.25722E-13
MSC	208090.3504	5.34039E-12
TMEM119	2160.255275	2.77334E-13
MKX	188322.4014	8.92952E-12
MMP19	184843.5577	9.82947E-12
SQRDL	3900.151926	2.70362E-12
GBP1	180205.0996	1.12035E-11

Table 2
Top 20 down-regulated genes in SMSCs versus iPSC-derived NPCs (iNPCs).

Top 20 down-regulated genes (SMSCs vs. iNPCs)		
Gene Symbol	**RealFC**	**PPEE**
SMA5	0.079	0.049
SLC37A1	0.076	0.049
STRIP2	0.078	0.048
PBK	0.078	0.049
SYT1	0.077	0.045
GDPD1	0.074	0.044
ZNF749	0.071	0.048
MEGF10	0.075	0.043
PLCG2	0.074	0.043
WDR17	0.076	0.044
FAM72B	0.074	0.041
ADGRB3	0.069	0.044
PRSS35	0.073	0.040
FAM65B	0.073	0.039
ZNF467	0.072	0.039
ATP2A1-AS1	0.068	0.042
ELMO1	0.069	0.041
LOC400927-CSNK1E	0.071	0.038
GINS2	0.074	0.041
PLCXD1	0.074	0.043

ther details of the results of the comparison of the differential gene expression involved in biological processes, molecular function, and cellular components between SMSCs and iPSC-derived NPCs.

3.3. Effects of SMSCs on chronic cisplatin treatment–induced hearing loss in mice

In this study, we investigated the effects of SMSCs on cisplatin-induced SHL in mice. To investigate the effects of cisplatin chronic toxicity in mice, we administered 4 mg/kg of cisplatin through IP injection once per day for 5 consecutive days (Fig. 3A). Chronic injection of cisplatin significantly reduced the body weight of mice in the treatment group ($P = 0.005$, Figs. 3B and 3C) compared with that of mice in the control group. Mice were treated 3 days after IP cisplatin injections with 1×10^6 or 3×10^6 SMSCs through tail vein injection. Our data suggested that treatment with 3×10^6 SMSCs increased the body weight of cisplatin-injected mice ($P = 0.04$, Figs. 3B and 3C). Furthermore, the cisplatin-injected mice exhibited greater increases in their hearing threshold (8 kHz, $P = 0.005$; 12 kHz, $P = 0.0001$) compared with the control mice (Fig. 3D). After tail vein injection of 3×10^6 SMSCs, cisplatin-injected mice had a hearing threshold of 23.33 ± 2.36 dB at 12 kHz, reflecting a reduction of approximately 10 dB (Figs. 3D and 3E). Moreover, we investigated the loss of HCs in the cochlear tissues of each group of mice through immunohistochemistry analysis. Anti-Myo7A antibody was used for immunofluorescence staining to examine the locations and numbers of OHCs and IHCs in the cochlear tissues of mice. Anti-phalloidin was used to stain the cytoskeleton and actin filaments of cochlear cells. Notably, as illustrated in Figs. 3F–3I, we observed a significant loss of Myo7A(+) OHCs in the middle and base regions of the cochlear tissues of cisplatin-injected mice. Moreover, in cisplatin-injected mice, injection of 1×10^6 or 3×10^6

Table 3
Up-regulated expression of stem cell marker genes or growth factor related genes in SMSCs versus iPSC-derived NPCs (iNPCs).

Up-regulated expression of stem cel marker genes or growth factor-related genes (SMSCs vs. iNPCs)		
Gene Symbol	**Real Fold Change**	**PPEE**
KLF4	13.729	0.015216344
SOX15	18.723	0.048270199
PAX8	16.618	0.011496776
WNT5A	35.681	0.000212488
WNT5B	51.417	3.04272E-05
WNT11	46.129	5.58332E-05
SLIT3	12.735	0.037484942
FGF1	239.284	3.96326E-06
FGF5	175.530	2.58546E-07
FGF7	2311.665	3.55815E-12
VEGFB	46.076	5.48468E-05
PTGS2	85.571	7.25815E-05
PDGFRA	63.356	1.16726E-05
PDGFRB	19.720	0.00458922
PDGFRL	33.725	0.000238301
PDGFD	75.188	4.72274E-06
NGF	102.814	1.97815E-06

Table 4
Down-regulated expression of stem cell marker genes or growth factor-related genes in SMSCs versus iPSC-derived NPCs (iNPCs).

Down-regulated expression of stem cell marker gene or growth factor-related genes (SMSCs vs. iNPCs)		
Gene Symbol	**Real Fold Change**	**PPEE**
SOX1	2.647E-05	2.5969E-06
SOX2	9.775E-04	1.80173E-08
SOX3	1.895E-05	7.31342E-07
SOX5	3.361E-05	6.38521E-06
SOX6	1.288E-02	0.000309006
SOX10	2.441E-05	1.91117E-06
SOX11	1.294E-03	3.56945E-08
SOX13	2.867E-02	0.001658553
SOX21	2.467E-04	0.008124711
PAX2	7.339E-05	0.000116396
PAX3	5.175E-02	0.015637796
PAX6	2.661E-02	0.001217488
PAX7	1.559E-05	3.48063E-07
WNT7A	1.999E-04	0.004040937
SLIT1	1.049E-06	1.12377E-11
FGF9	8.282E-05	0.000181031
FGF11	4.821E-03	5.37502E-06
FGF13	7.346E-02	0.04137858
FGFR2	1.243E-03	2.37516E-08
FGFR3	5.519E-03	3.98064E-06
FGFR4	4.709E-02	0.009708168
KDR	9.216E-03	8.96683E-05
FLT4	4.171E-05	1.43503E-05
IGF2	1.165E-02	6.40126E-05

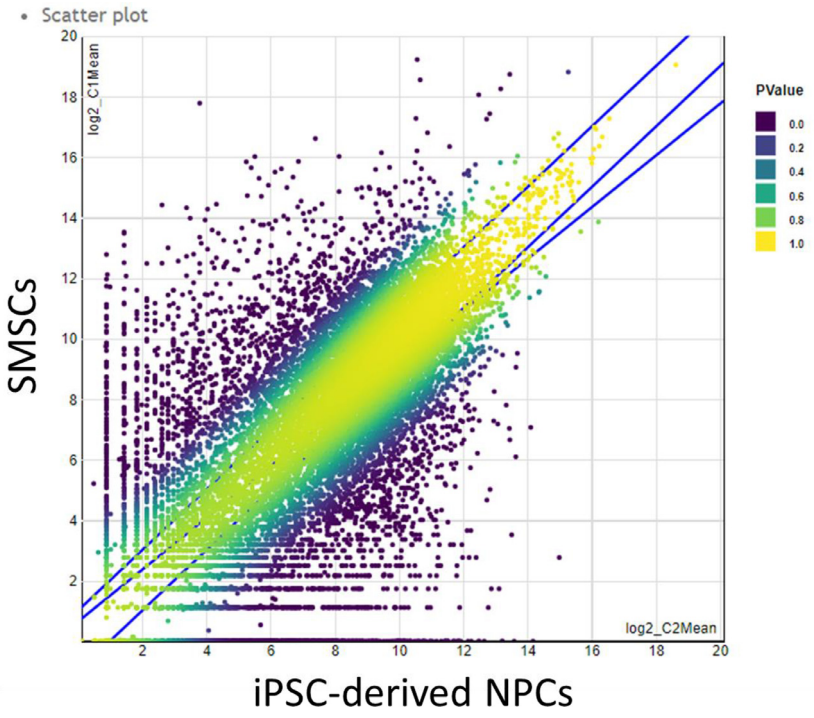

Fig. 2. Whole transcriptome analyses of human SMSCs using RNA sequencing technology. (A) Scatter plot of the results from RNA-seq analyses of SMSCs and human iPSC-derived NPCs (iPSC-derived NPCs). (B) Top 20 upregulated and downregulated genes in SMSCs versus in iPSC-derived NPCs. EBseq analysis was used for the RNAseq differential expression. PPEE is the posterior probability of equal expression, indicating that a gene/transcript is equally expressed. (C) Representative upregulated genes of stem cell markers or growth factors in SMSCs compared with in iPSC-derived NPCs. (D) Representative downregulated genes of stem cell markers or growth factors in SMSCs compared with in iPSC-derived NPCs.

SMSCs significantly mitigated the loss of Myo7A(+) OHCs in the middle and base regions of the cochlear tissues (Figs. 3F–3I).

3.4. Effects of SMSCs on acute-cisplatin treatment–induced hearing loss in mice

For the cisplatin acute toxicity experiment, we used a 25 mg/kg dose for the IP injection on day 1 (Fig. 4A). Mice were then treated with 1×10^6 or 3×10^6 SMSCs through tail vein injection 3 days after cisplatin injections. Our data indicated no difference in body weight among mice in the control, acute-cisplatin injection, and SMSC treatment groups (Fig. 4B). Furthermore, an increase in the hearing threshold was observed in mice that received acute-cisplatin injection compared with the control mice (Fig. 4C). In mice exposed to cisplatin, injection of 3×10^6 SMSCs resulted in about 10 dB reduction of the hearing thresholds measured at 12 kHz (Figs. 4C and 4D). Additionally, as displayed in Figs. 4E–4H, cisplatin-injected mice exhibited a significant loss of Myo7A(+) OHCs in the length of 300 μm of apex, middle, and base regions in the cochlear tissues. In cisplatin-injected mice, injection of 3×10^6 SMSCs moderately mitigated the loss of Myo7A(+) OHCs in the middle and base regions of the cochlear tissues (Figs. 4E–4H).

3.5. Neuropathological gene expression analysis revealed dysregulation in the mouse cochlear tissues after acute-cisplatin and SMSC treatments

We selected three representative samples from our ABR experiments for NanoString gene expression analyses in each group, as follows: control (n = 3, hearing threshold of 10 dB for all three at 12 kHz), cisplatin (n = 3, hearing thresholds of 50, 50, and 70 dB at 12 kHz), and cisplatin + 3×10^6 SMSCs (n = 3, hearing threshold of 20 dB for all three at 12 kHz). A NanoString neuropathology panel was used to analyze the relative RNA abundance of the three representative cochlear samples in each group. The analysis identified many genes involved in important neuropathological pathways that were clustered, which enabled evaluation of the damaging effects of cisplatin on cochlear tissues and the beneficial effects of SMSCs on the damaged cochlea (Figs. 5A–5C). Data of the gene scores for the cochlear tissue of cisplatin-injected mice indicated upregulation of genes involved in apoptosis, autophagy, chromatin modification, disease association, matrix remodeling, oxidative stress, tissue integrity, transcription, splicing, and unfolded protein responses. Notably, in cisplatin-injected mice, the abnormal transcriptional pattern could be reversed by treatment with 3×10^6 SMSCs (Figs. 5A–5C). Furthermore, the gene scores for the cochlear tissues of cisplatin-injected mice revealed the downregulation of genes affecting the axon and dendrite structure, cytokines, the neuronal skeleton, and trophic factors and those involved in carbohydrate metabolism, growth factor signaling, myelination, neural connectivity, neural transmitter release, neural transmitter response and reuptake, neural transmitter synthesis and storage, and vesicle trafficking. Notably, the abnormally downregulated gene scores in cisplatin-injected mice could be effectively reversed by treatment with 3×10^6 SMSCs (Fig. 5C). To investigate whether SMSCs could reduce cell apoptosis in the cochlear tissues of cisplatin-injected mice, we analyzed apoptosis by TUNEL and cleaved caspase-3 stainings. Increased TUNEL-positive cells were observed is the apex, middle and base region of cochlear tissues of cisplatin-injected mice. Notably, SMSCs treatment could reduce the TUNEL-positive cells in apex, middle and base region of cochlear tissues, indicating that SMSCs treatment could reduce cisplatin-induced apoptosis in cochlear tissues (Fig. 5D). Furthermore, our results showed that number of cleaved caspase-3/Myo7a double-positive cells was significantly increased base region of cochlear tissues from cisplatin-injected mice (Fig. 5G). Interest-

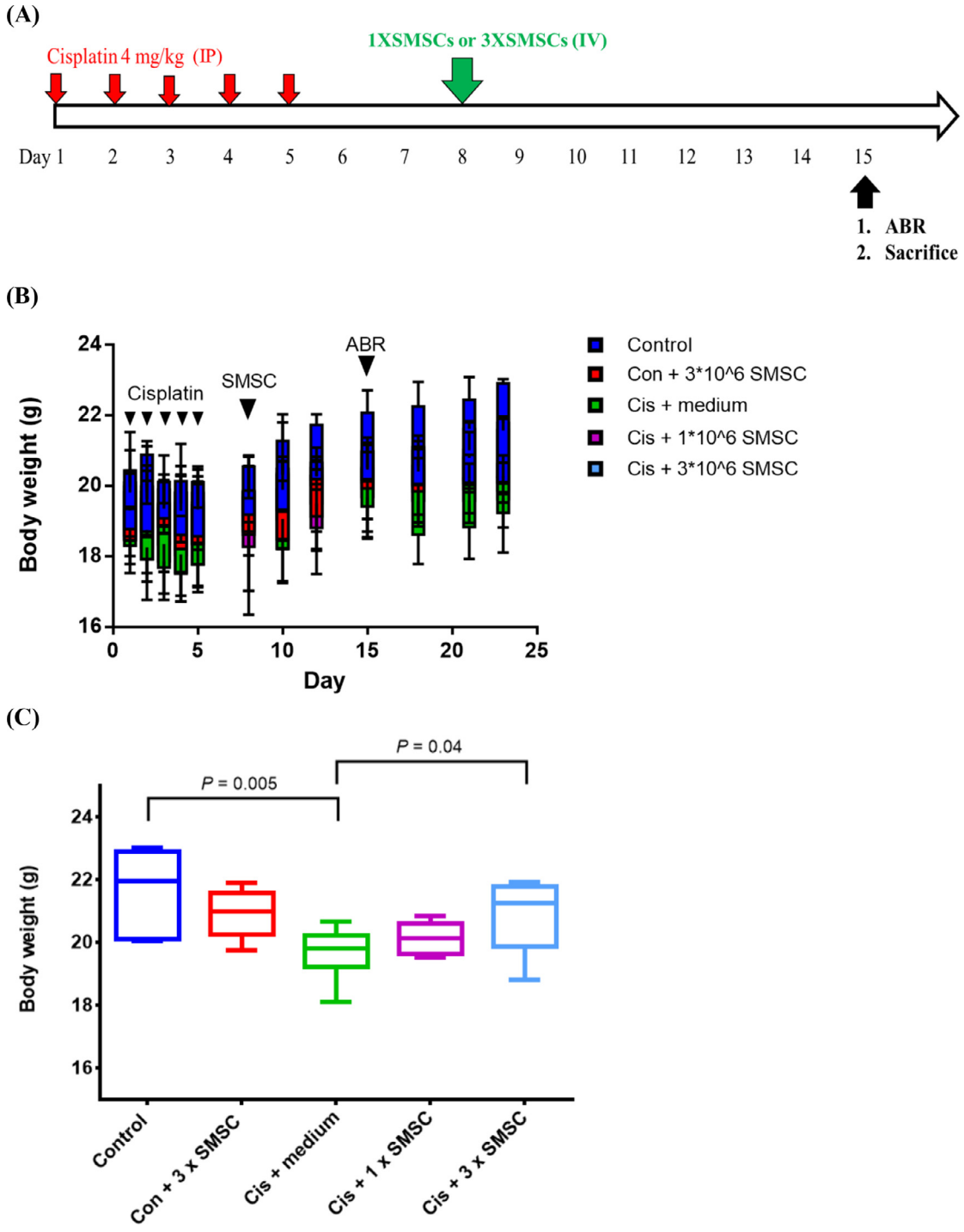

Fig. 3. Effects of SMSCs on the chronic cisplatin–induced hearing loss in mice. (A) Schematic of the experimental design of chronic cisplatin administration for inducing hearing loss in mice. Mice received intraperitoneal injection of cisplatin (4 mg/kg) once per day for 5 consecutive days. 1xSMSCs (1×10^6) and 3xSMSCs (3×10^6) were administered through tail vein injection 3 days later. One week later, the hearing threshold of all groups of mice was measured using an auditory brain response (ABR) instrument. After ABR measurement, mice were sacrificed to obtain cochlear tissues for immunohistochemical staining. (B) Results of analysis of the body weights of all mice groups. (C) The cisplatin-injected mice that received 3×10^6 SMSC treatment had higher median body weight compared with the cisplatin-injected mice without SMSC treatment; $P = 0.04$, n = 6–9 in each group. (D) The results of ABR measurements showed that cisplatin-injected mice had significantly impaired hearing function at the frequencies of 8 and 12 kHz compared with the control group. After 3×10^6 SMSC treatment, the hearing threshold of the cisplatin-injected mice at 8 and 12 kHz was reduced by 30% (approximately 10 dB) compared with that of cisplatin-injected mice that did not receive SMSC treatment; n = 6–9 in each group. (E) Representative results of ABR at the frequency of 12 kHz in each group. (F) The results for the outer hair cell (OHC) loss of cochlear tissues showed that cisplatin-injected mice had a significant loss of OHCs in the apex, middle, and base regions compared with the control group. After 1×10^6 or 3×10^6 SMSC treatment in cisplatin-injected mice, the loss of OHCs in the middle and base regions was significantly reduced compared with that of the cisplatin-injected mice that received no SMSC treatment; n = 6–9 in each group. (G) Representative results of immunohistochemical staining of the nucleus (DAPI, blue), hair cells (HCs, Myo7A, red), and cytoskeleton (phalloidin staining, green) in the apex region of the cochlear tissues in each group of mice. Scale bar = 25 μm. Arrows indicate the loss of OHCs in the cochlear tissues. (H) Representative results of immunohistochemical staining in the middle region of the cochlear tissues in each group of mice. Scale bar = 25 μm. (J) Representative results of immunohistochemical staining at the base region of the cochlear tissues in each group of mice. Scale bar = 25 μm. Abbreviations: Con + 3xSMSCs = Control + 3×10^6 SMSCs; Cis + med = Cisplatin + medium; Cis + 1xSMSCs = Cisplatin + 1×10^6 SMSCs; Cis + 3xSMSCs = Cisplatin + 3×10^6 SMSCs. Bonferroni correction was used for multiple analysis. Statistical significance was defined as $P < 0.005$ in the experiments of Figure 3.

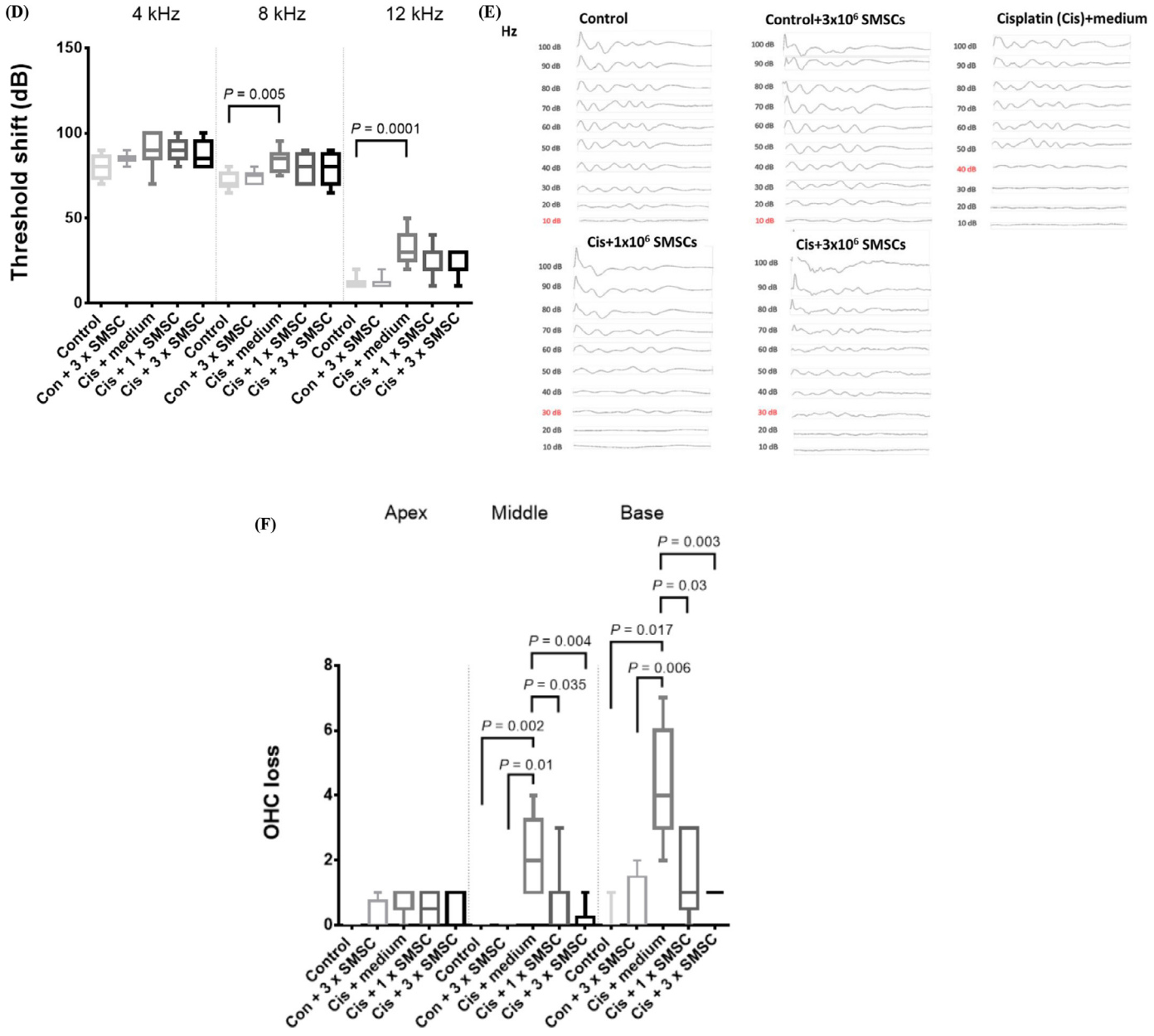

Fig. 3. Continued

ingly, we observed that cleaved caspase-3 was expressed more in supporting cells than Myo7a(+) cells in apex and middle regions of cochlear tissues from cisplatin-injected mice (Figs. 5E and 5F). Moreover, SMSCs treatments could reduce the cleaved caspase-3/Myo7a double-positive cells in the base regions (Fig. 5G) and cleaved caspase-3-positive cells in middle and apex regions (Figs. 5E and 5F) of cochlear tissues from cisplatin-injected mice. The data from TUNEL and the cleaved caspase-3 stainings are consistent with the findings of apoptosis gene score suggested by NanoString neuropathological gene panel (Fig. 5A).

3.6. Cell-type specific gene expression analysis revealed the relative abundance of different cell types in mouse cochlear tissues after acute-cisplatin and SMSC treatments

Typical cell marker genes of neurons, astrocytes, Schwann cells, endothelial cells (ECs), and microglial cells were clustered; neuropathological gene expression panel analyses were performed to evaluate the damaging effects of cisplatin on the cochlear tissues and the beneficial effects of SMSCs on the damaged cochlea (Fig. 6A). Our data revealed that astrocytes and ECs in the cochlear tissues of cisplatin-injected mice had increased marker gene expression levels. SMSC treatment could mitigate the increase in marker gene expression levels in astrocytes, microglial cells, and ECs in the cochlear tissues of cisplatin-injected mice (Fig. 6B-i). By contrast, decreased marker gene expression levels were observed in the neurons and oligodendrocytes in the cochlear tissues of cisplatin-injected mice. SMSC treatment could increase the mRNA expression levels of neurons and oligodendrocytes in the cochlear tissues of cisplatin-injected mice (Fig. 6B-ii).

4. Discussion

The present study investigated the SMSC transcriptome and demonstrated the protective effects of the IV administration of SM-

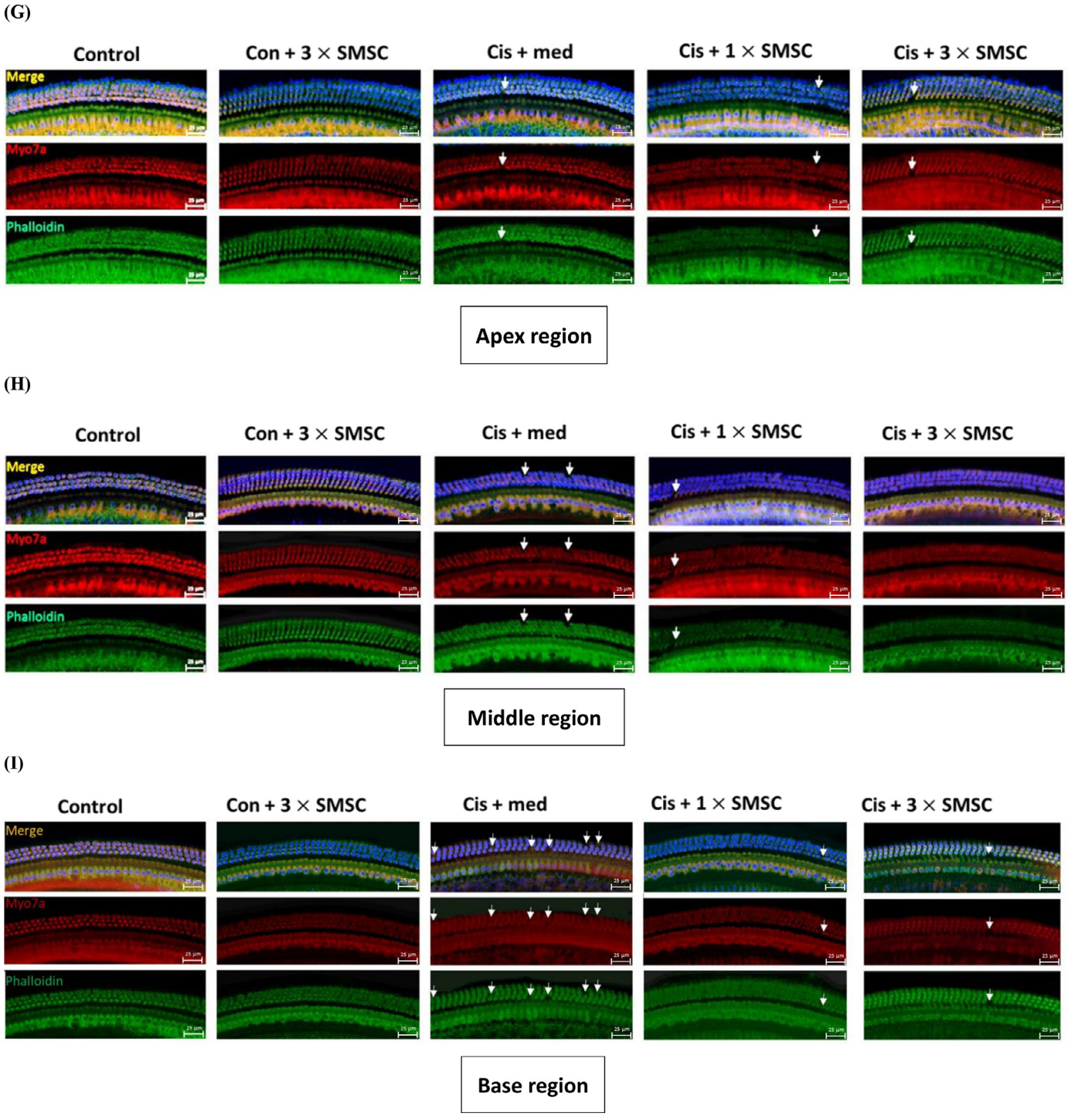

Fig. 3. Continued

SCs on cisplatin-induced ototoxicity in mice. According to our data, SMSCs could be differentiated not only into adipocytes, osteoblasts, chondrocytes (Fig. 1B), but also into NeuN(+) and Map2(+) neurons (Fig. 1C), indicating that SMSCs possess not only MSC differentiation capacity but also possess similar differentiation capacity to that of neural precursor cells (NPCs). Moreover, SMSCs used in this study were positive for the cell surface markers of CD73, CD90, and CD105 (Fig. 1B), which have been demonstrated to be definitive markers of MSCs (Nold et al., 2019). Notably, CD73(+)/CD90(+)/CD105(+) MSCs from adipose tissues (Jahanbazi Jahan-Abad et al., 2017) or BM (Singh et al., 2013) can be differentiated into neurons. These adipose MSCs can further form neurospheres that also express *NESTIN*, *SOX2*, *GFAP*, and *MAP2* (Jahanbazi Jahan-Abad et al., 2017). Since SMSCs possess the differentiation capacity to NeuN(+) and Map2(+) neurons in vitro. Therefore, it is of great interests to compare the transcriptomes between SMSCs and NPCs. Since human primary NPCs is very difficult to obtain, we chose to make use of human iPSCs-derived NPCs. As displayed in Table 3, transcriptome analyses revealed that the mRNA expression profile of SMSCs included the embryonic stem cell marker genes *KLF4* (Aksoy et al., 2014) and *SOX15* (Maruyama et al., 2005) and the NPC marker gene *PAX8* (Ahn et al., 2004). Furthermore,

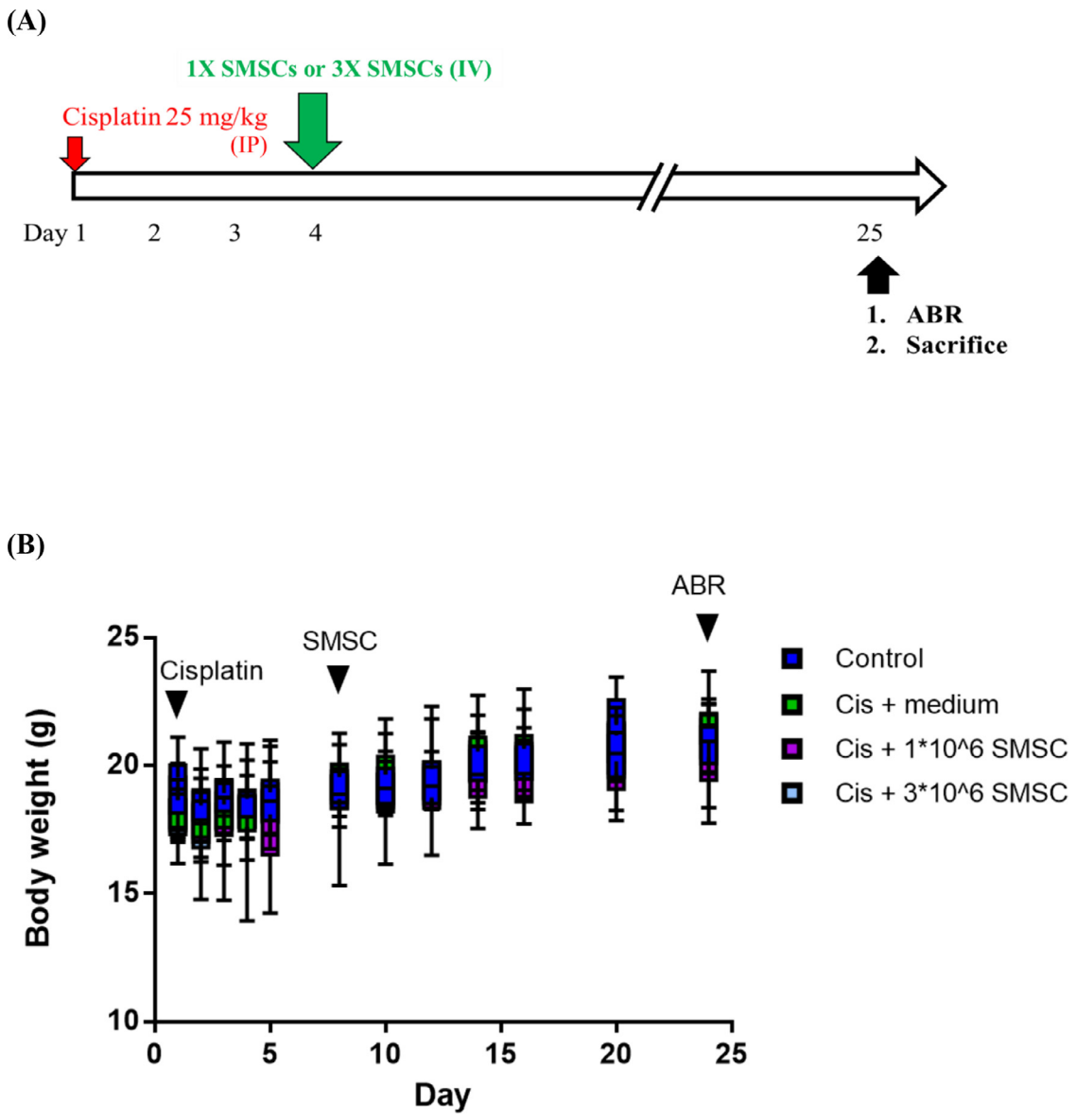

Fig. 4. Effects of SMSCs on acute-cisplatin–induced hearing loss in mice. (A) Schematic of the experimental design of chronic administration of cisplatin for inducing hearing loss in mice. Cisplatin (25 mg/kg) was injected intraperitoneally once on the first day. SMSCs (1×10^6 and 3×10^6) were administered through tail vein injection 3 days later. After 3 weeks, the hearing threshold of all groups of mice was measured using an ABR instrument. After ABR measurement, mice were sacrificed to obtain cochlear tissues for immunohistochemical staining. (B) No significant difference in body weight was observed among the mice groups; n = 7–10 in each group. (C) The results of ABR measurement showed that cisplatin-injected mice had significantly impaired hearing function at the frequency of 12 kHz compared with mice in the control group ($P = 0.01$). After 3×10^6 SMSC treatment in cisplatin-injected mice, the hearing threshold at 12 kHz was significantly reduced compared with that of the cisplatin-injected mice without SMSC treatment, $P = 0.026$. (D) Representative results of ABR at the frequency of 12 kHz for each group of mice. (E) The results for OHC loss of cochlear tissues indicated that cisplatin-injected mice had a significant loss of OHCs in the middle and base regions compared with the control group; $P = 0.038$ and $P = 0.038$, respectively. After 1×10^6 and 3×10^6 SMSC treatment in cisplatin-injected mice, the loss of OHCs in the middle and base regions was moderately reduced compared with that of the cisplatin-injected mice without SMSC treatment. (F) Representative results of immunohistochemical staining of the nucleus (DAPI, blue), hair cells (HCs, Myo7A, red), and cytoskeleton (phalloidin staining, green) in the apex region of the cochlear tissues in each group of mice. Scale bar = 25 μm. Arrows indicate the loss of OHCs in the cochlear tissues. (G) Representative results of immunohistochemical staining in the middle region of the cochlear tissues in each group of mice. Scale bar = 25 μm. (H) Representative results of immunohistochemical staining in the base region of the cochlear tissues in each group of mice. Abbreviations: Cis + med = Cisplatin + medium; Cis + 1xSMSCs = Cisplatin + 1×10^6 SMSCs; Cis + 3xSMSCs = Cisplatin + 3×10^6 SMSCs. Bonferroni correction was used for multiple analysis. Statistical significance was defined as $P < 0.008$ in the experiments of Figure 4.

Figs. 2B and 2C show that SMSCs could express the mRNAs of multiple growth factor genes, including *VEGFB* (Monastero et al., 2017; Sun et al., 2006), *FGF2* (Kleiderman et al., 2016), *PDGFD* (Uutela et al., 2001), and *NGF* (Wang et al., 2019). Evidence suggests that different types of stem and progenitor cells, such as MSCs (Ahn et al., 2004), NPCs (Andsberg et al., 1998), and otic progenitor cells (OPCs) (Vemaraju et al., 2012), can secrete multiple growth factors for the repair of different tissues in various organ systems. The growth factor expression profile may account for the effects of SMSCs on cochlear tissue repair (Figs. 2C). Notably, Wnt signaling is crucial for Lgr5(+) to support cell maintenance in the cochlea, which is responsible for the regeneration of cochlear HCs (Li et al., 2015b). In this study, SMSCs expressed *WNT5A*, *WNT5B*, and *WNT11* mRNAs (Figs. 2C), indicating that the

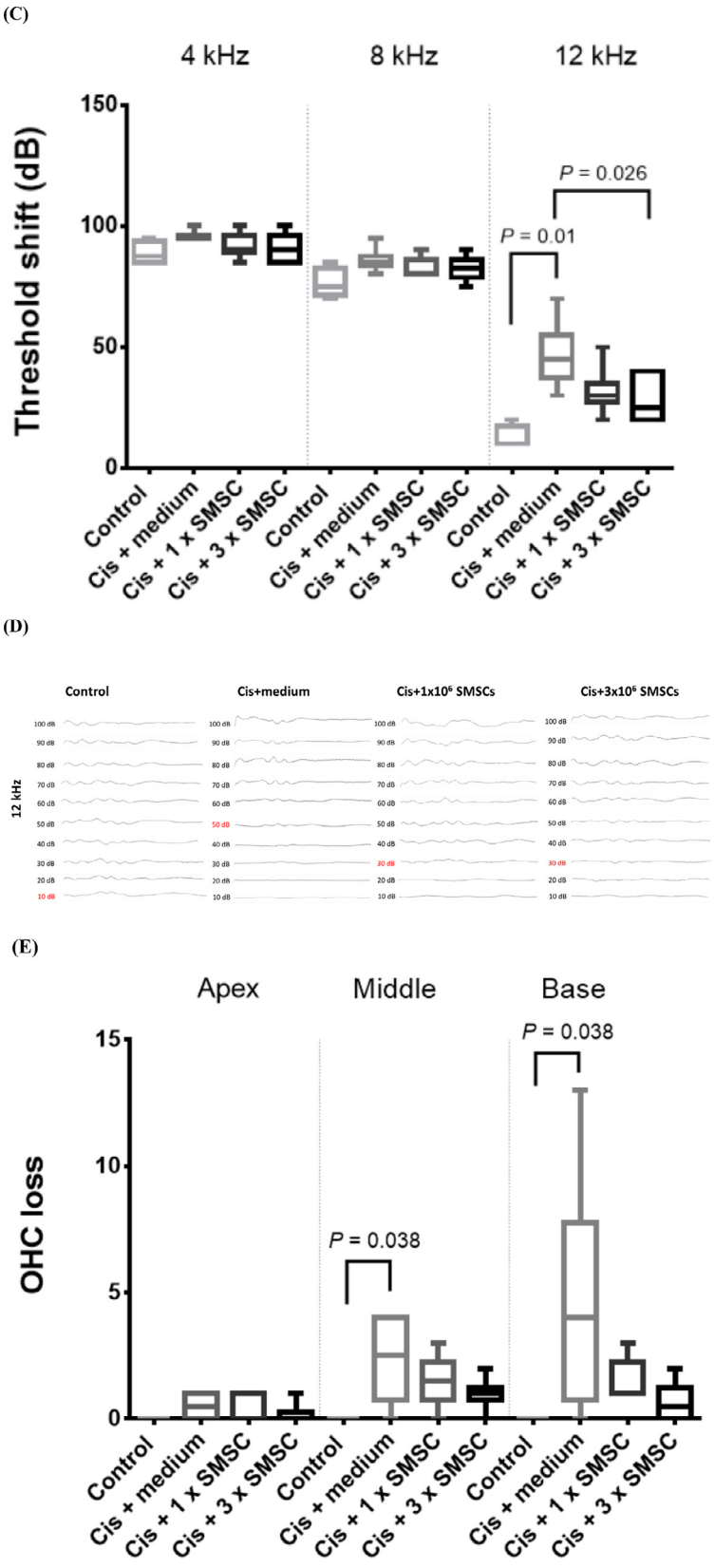

Fig. 4. Continued

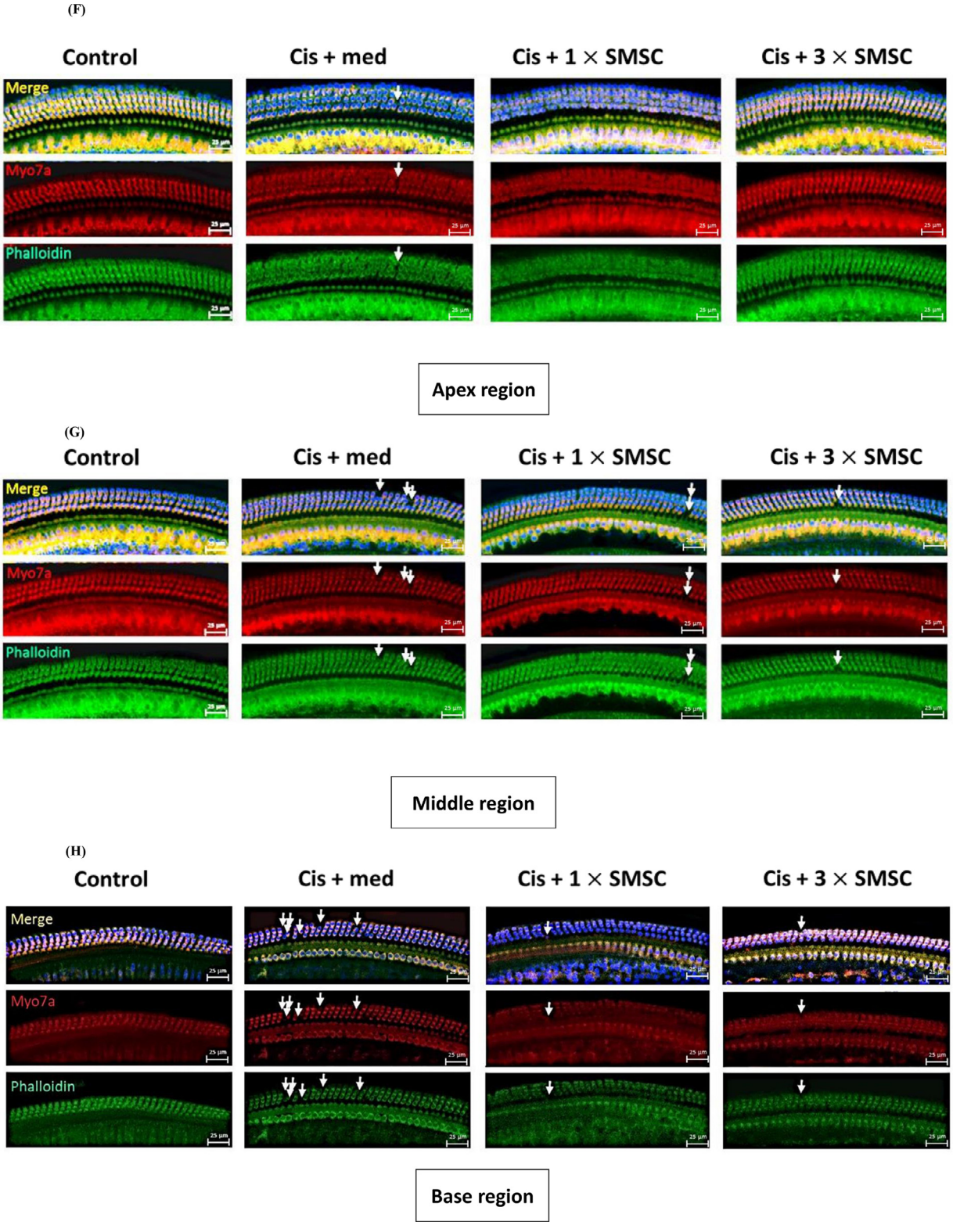

Fig. 4. Continued

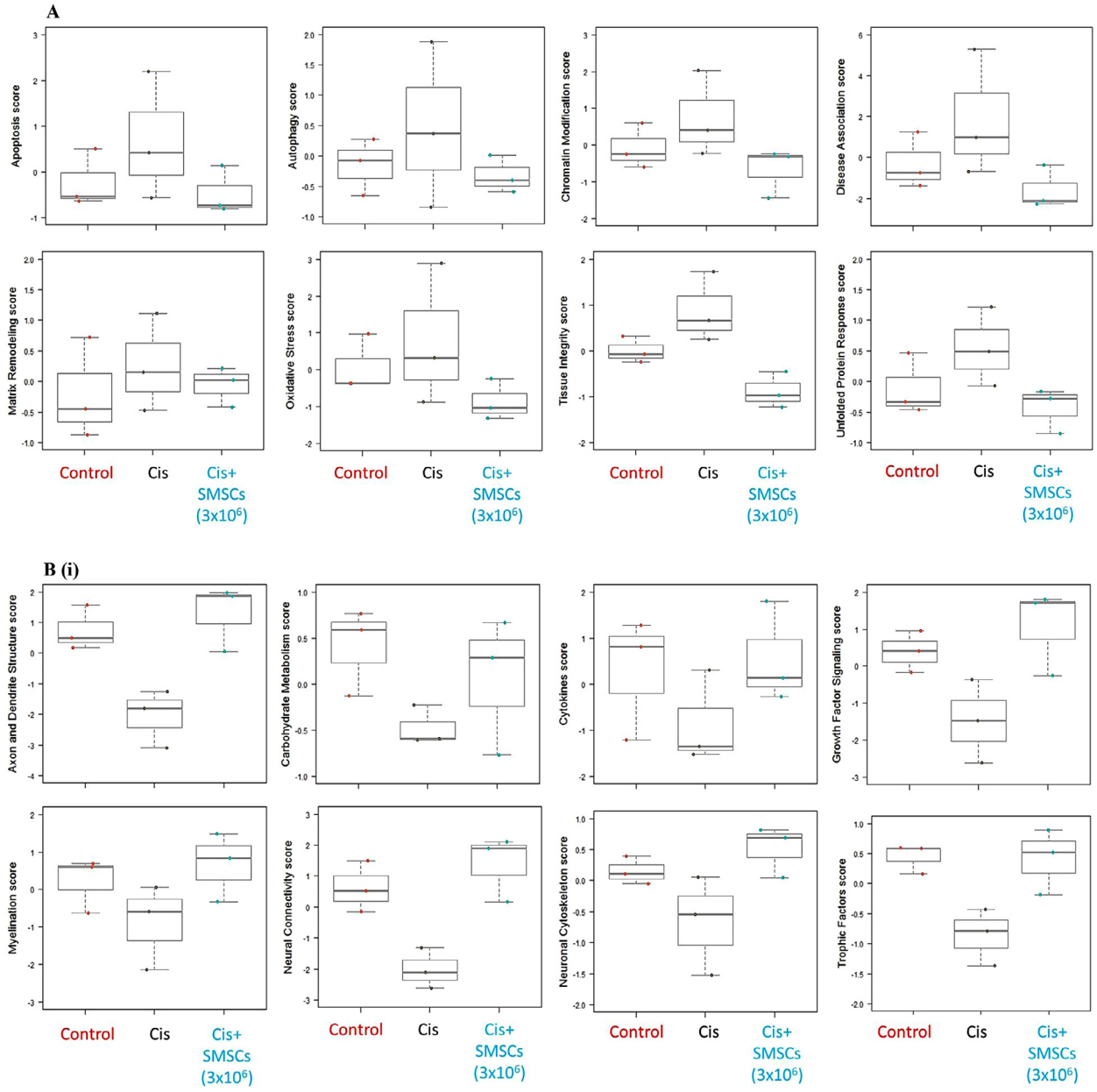

Fig. 5. Neuropathological gene panel analyses of the protective effects of SMSCs against cisplatin-induced hearing loss in mice. (A) Increases in the gene scores of biological pathways in the mRNA expression profiles of the cochlear tissues in three representative mice that received acute-cisplatin injection. SMSC treatment reduced the gene scores of biological pathways. (B) Decreases in the gene scores of biological pathways in the mRNA expression profiles of the cochlear tissues in three representative mice that received acute-cisplatin injection. SMSC treatment increased the gene scores of biological pathways. (C) Heat map of the gene expression profiles for each biological pathway after normalization with the control group: cisplatin vs. control (ctrl) and 3 × SMSCs (cisplatin mice treated with 3×10^6 SMSCs) vs. ctrl. (D) Immunofluorescence staining with TUNEL in the apex, middle and base regions of the cochlear tissues from different groups. Immunofluorescence staining results with cleaved caspase-3 in the apex (E), middle (F) and base (G) regions of the cochlear tissues from different groups are shown.

properties of stem and progenitor cells are preserved during WNT signaling.

In the present study, we described SMSCs' transcriptome and showed protective effects of systemic administration of SMSCs on cisplatin-induced ototoxicity in mice. Other researchers have also used cisplatin (25 mg/kg) to induce acute nephrotoxicity within 3 days (Yang et al., 2020; Zhang et al., 2020; Zhou et al., 2020). To clarify whether the effects of SMSCs are exerted through protection against nephrotoxicity, we also evaluated the effects of SMSCs on nephrotoxicity. An acute dose of cisplatin (25 mg/kg) did not appar to affect the kidney weight of the cisplatin-treated mice, according to measurements taken after they were sacrificed. Furthermore, neither cisplatin nor SMSC treatment affected the levels of serum biochemical markers, such as aspartate transaminase, alanine aminotransferase, creatinine, and total bilirubin (Supplementary Fig. 2). We also evaluated the pathological scores for kidney sections of mice in all groups and did not observe any significant differences (data not shown). Therefore, our results suggest that the effects of SMSCs may be exerted not only through protection against nephrotoxicity, but also through protection against hearing loss; specifically, SMSCs may have reduced nephrotoxicity in mice

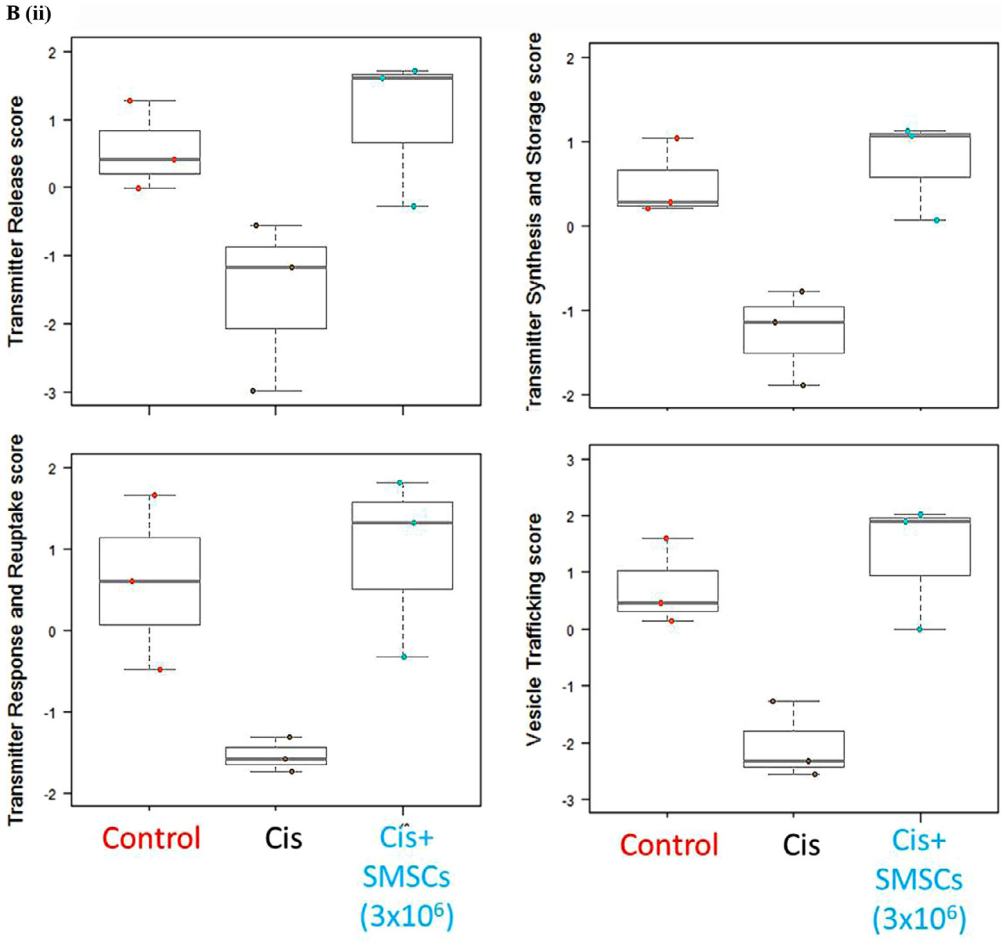

Fig. 5. Continued

within the first week and may then exert protective effects against hearing loss on day 25.

Through bioinformatics analyses, we further compared the transcriptomes between SMSCs and iPSC-derived NPCs. Compared with iPSC-derived NPCs, SMSCs expressed higher expression levels of genes involved in enhancing biological processes, such as blood vessel morphogenesis, extracellular matrix and structure organization, angiogenesis, epithelial cell proliferation, and axon development (Supplementary Fig. 1A). At the molecular level, compared with iPSC-derived NPCs, SMSCs had higher expression levels of genes involved in glycosaminoglycan binding, heparin binding, transmembrane ion transport, and ion channel activities (Supplementary Fig. 1B). At the cellular level, compared with iPSC-derived NPCs, SMSCs had higher expression levels of genes affecting axons, neuronal cell bodies, and dendrites (Supplementary Fig. 1C). Overall, the characteristics of SMSCs differ from those of NPCs (Andsberg et al., 1998) and OPCs (Shi et al., 2012).

The results of the two independent experiments conducted in this study provide consistent evidence of the protective effects of SMSCs. SMSCs could improve hearing function and rescue the loss of OHCs (Figs. 3 and 4). Choi et al. reported that engrafting human MSCs to cochlear regions induced the expression of brain-derived neurotrophic factor; MSCs were located near degenerated IHCs and SGNs after intravenous injection into rats with noise- and drug-induced hearing loss (Choi et al., 2012; Kasagi et al., 2013). BM-derived MSCs can be successfully transplanted into the cochlea of young mice but spontaneously differentiated into fibrocyte-like cells with Cx26 expression and did not affect the auditory function of mice. (Kil et al., 2016) further demonstrated that placenta-derived MSCs could significantly improve hearing function in deaf animals, measured according to ABR and distortion-product otoacoustic emissions, and reported an increased number of SGNs in the cochlea and no apparent adverse effects or immunological rejection.

Data from the neuropathological gene expression panel provide valuable insight into the effects of SMSCs on cisplatin-induced hearing loss in mice (Figs. 5 and 6). For example, gene scores indicated the upregulation of genes involved in apoptosis, autophagy, and oxidative stress and the downregulation of genes affecting axon and dendrite structure, myelination, neural connectivity, and neural transmitters in the cochlear tissues of cisplatin-treated mice. Thus, the results of all of the gene expression analyses indicate favorable mRNA changes in the cochlear tissues of all groups. However, further immunohistochemistry examination is necessary for determining the cell types involved in cochlear injury. Notably, the expression of genes encoding proteins involved in oxidative stress, apoptosis, autophagy, chromatin modification, matrix remodeling, tissue integrity, transcription and splicing, and unfolded protein responses was upregulated in the cochlear tissues of cisplatin-injected mice (Fig. 5A). Cisplatin has been demonstrated to induce apoptosis in cochlear HCs through oxidative stress (Kikkawa et al., 2009), but PINK1-induced autophagy and downregulation of the JNK pathway can protect HCs from apoptosis (Yang et al., 2015). In the present study, our analyses revealed

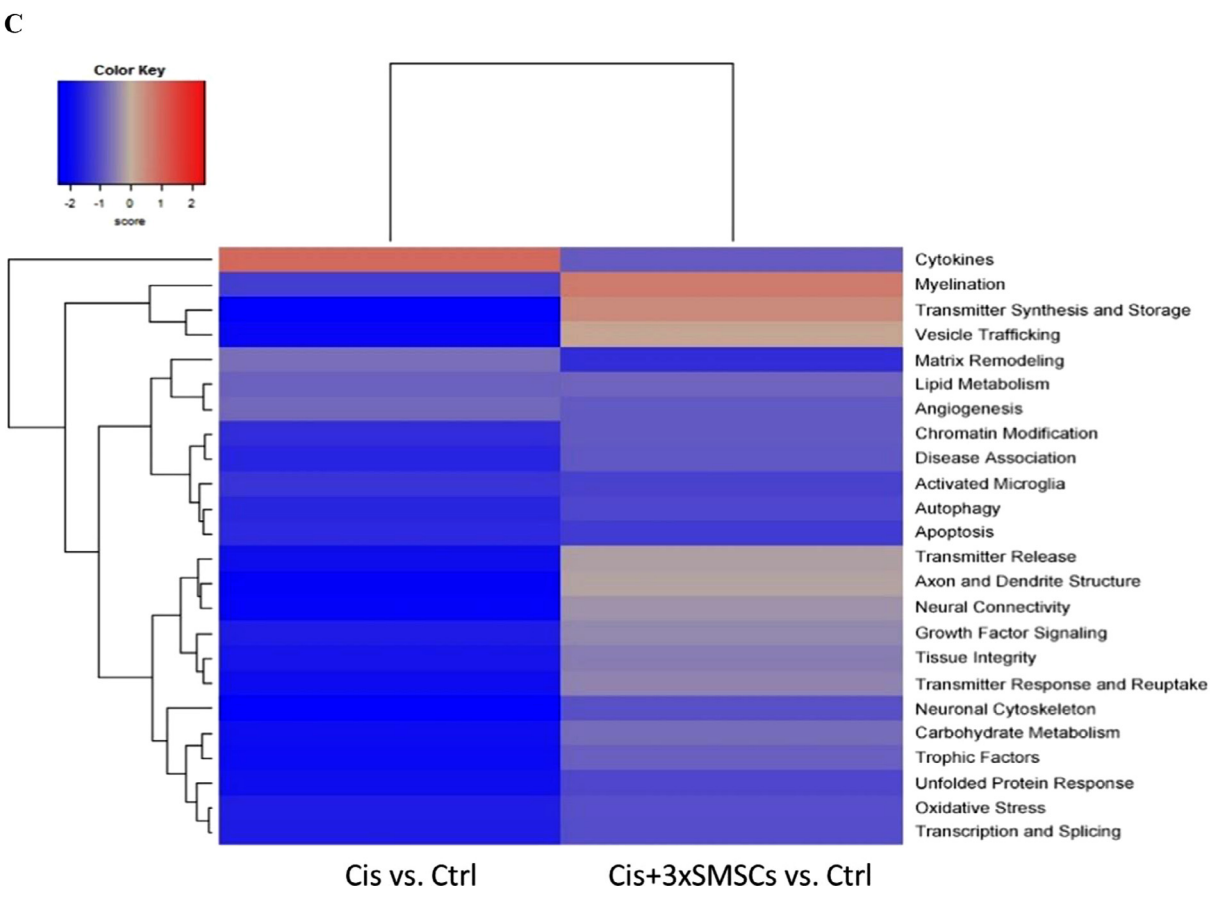

Fig. 5. Continued

that the regulation of chromatin modification, matrix remodeling, tissue integrity, transcription, and splicing and unfolded protein responses might also contribute to the ototoxicity of cisplatin. Fig. 5B shows the downregulated expression of genes in the cochlear tissue of cisplatin-injected mice. These genes include those encoding proteins that affect the axon and dendrite structure, trophic factors, the neuronal skeleton, and cytokines and those involved in carbohydrate metabolism, growth factor signaling, myelination, neural connectivity, neural transmitter release, neural transmitter response and reuptake, neural transmitter synthesis and storage, and vesicle trafficking. Cisplatin treatment has been demonstrated to induce SGN damage (Bowers et al., 2002) and the dysfunction of auditory nerves (Meen et al., 2010). This is consistent with our findings that cisplatin treatment can damage the axon and dendrite structure, cytokines, trophic factors, and the neuronal skeleton and impair carbohydrate metabolism, growth factor signaling, myelination, neural connectivity, neural transmitter release, neural transmitter response and reuptake, neural transmitter synthesis and storage, and vesicle trafficking (Figs. 5B and 5C). After normalization with the control group, our data suggest that SMSC treatment could reverse abnormalities induced by cisplatin in cochlear tissues (Figs. 5A-5C). The results of all of the gene expression analyses indicate possible mRNA changes in the cochlear tissues of all groups, and further immunohistochemistry examination is necessary for confirmation.

Our RNA-seq data indicate that SMSCs have mRNA expression patterns distinct from those of iPSC-derived NPCs for *SOX*, *PAX*, *WNT*, *VEGF*, *PDGF*, *FGFs* and *NGF* genes (Table 3) and that SMSCs and iPSC-derived NPCs have different characteristics of stem and progenitor cells (Fig. 2 and Supplementary Fig. 1). Regarding the in vivo efficacy of SMSCs, our data suggest that SMSCs have beneficial effects in terms of improved gene score for various genes, specified as follows. Firstly, affecting genes involved in oxidative stress, apoptosis, autophagy, chromatin modification, matrix remodeling, tissue integrity, transcription and splicing, and unfolded protein responses (Fig. 5A). Secondly, affecting genes involved in axon and dendrite structure, cytokines, trophic factors, and the neuronal skeleton and involved in carbohydrate metabolism, growth factor signaling, myelination, neural connectivity, neural transmitter release, neural transmitter response and reuptake, neural transmitter synthesis and storage, and vesicle trafficking (Fig. 5B). Thirdly, affecting genes involved in axon and dendrite structure, cytokines, the neuronal skeleton, and trophic factors and affecting genes involved in carbohydrate metabolism, growth factor signaling, myelination, neural connectivity, neural transmitter release, neural transmitter response and reuptake, neural transmitter synthesis and storage, and vesicle trafficking (Fig. 5C). These findings may be highly correlated with gene expression profile of SMSCs (Fig. 2 and Supplementary Fig. 1).

Furthermore, the results of our data in cell type-specific gene score analysis suggest that astrocytes and ECs are upregulated in the cochlear tissues of cisplatin-injected mice (Fig. 6). Notably, GFAP-positive astrocytes can migrate, and their processes can extend across the central nervous system transitional zone along the cochlear nerves following neomycin-induced SHL in mice, suggesting that GFAP-expressing astrocytes migrate across from central nervous system to the peripheral nervous system (Hu et al., 2014). Furthermore, it has been reported microglial activation and prolif-

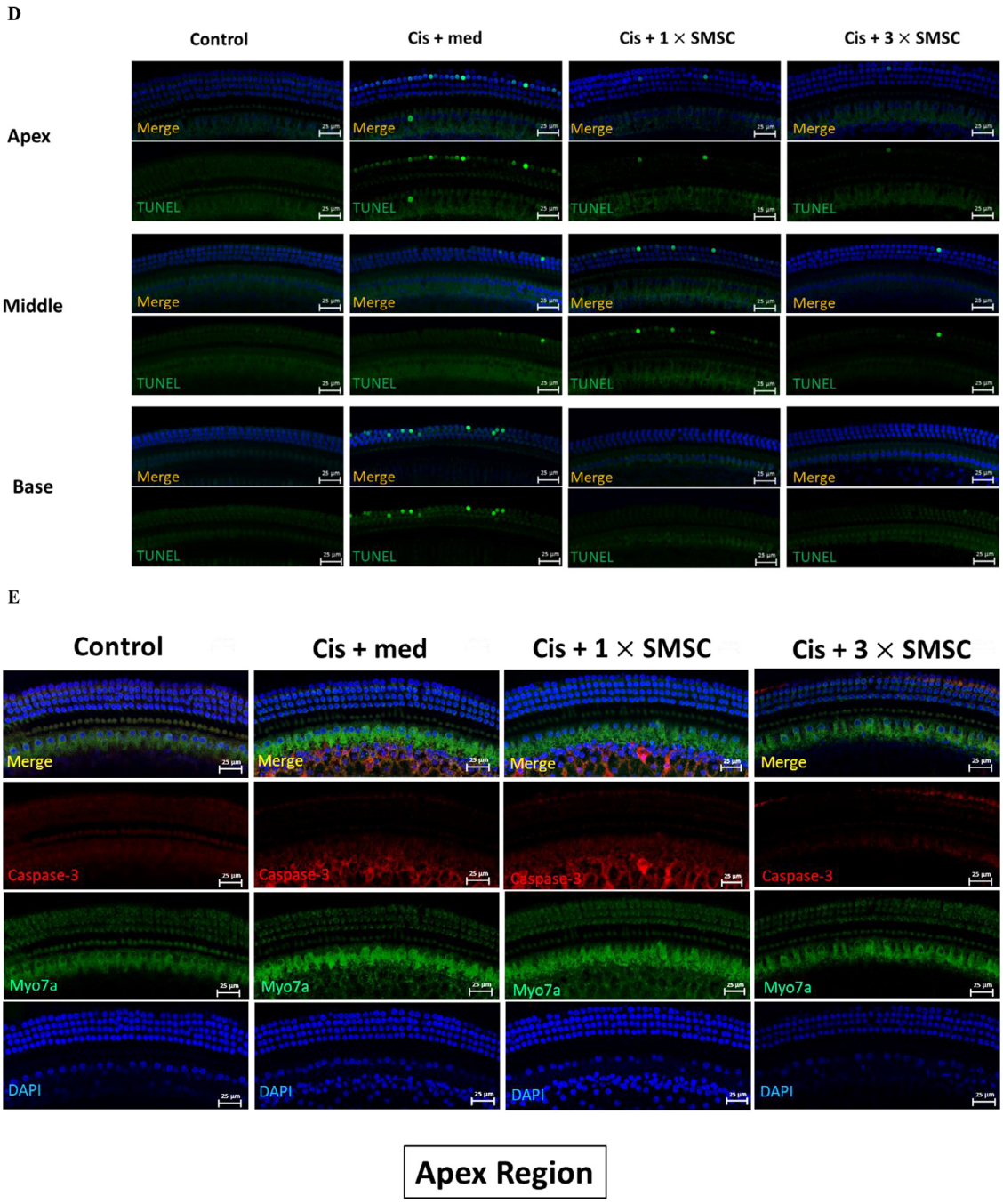

Fig. 5. Continued

eration in the cochlear nucleus, indicating that microglial cells play role in noise-induced hearing loss (Noda et al., 2019). Additionally, in mice with noise-induced hearing loss, the number of circulating endothelial progenitor cells and expression level of VEGF are increased, exerting a neoangiogenic effect (Yang et al., 2015). Cisplatin treatment can downregulate neurons and Schwann cells (Fig. 6), which may account for the neuronal and myelination abnormalities apparent in Fig. 5B. Consequently, SMSC treatment could reverse abnormal changes in different types of cells in the cochlear tissues of cisplatin-injected mice (Fig. 6). Taken together, our findings suggest that SMSCs exert protective effects against cisplatin-induced hearing loss in mice.

The present study had some limitations, such as (i) limited audiometric data; (ii) pathway or cell type specific scores should be interpreted with caution. The scores may be confounded by biological effects (i.e., proliferation or immune cell abundance) or technical effects (i.e., sample input or preparation) unrelated to the pathway activity. Further immunohistochemistry examination is necessary for confirmation; (iii) the RNA-seq comparison data of SMSCs and iPSC-derived NPCs were not further validated by another method; (iv) the lack of a clearer explanation of the mechanism: a deeper histologic study tracking labeled SMSC in the cochlea would show migration to the cochlea and support a direct effect as a potential mechanism.

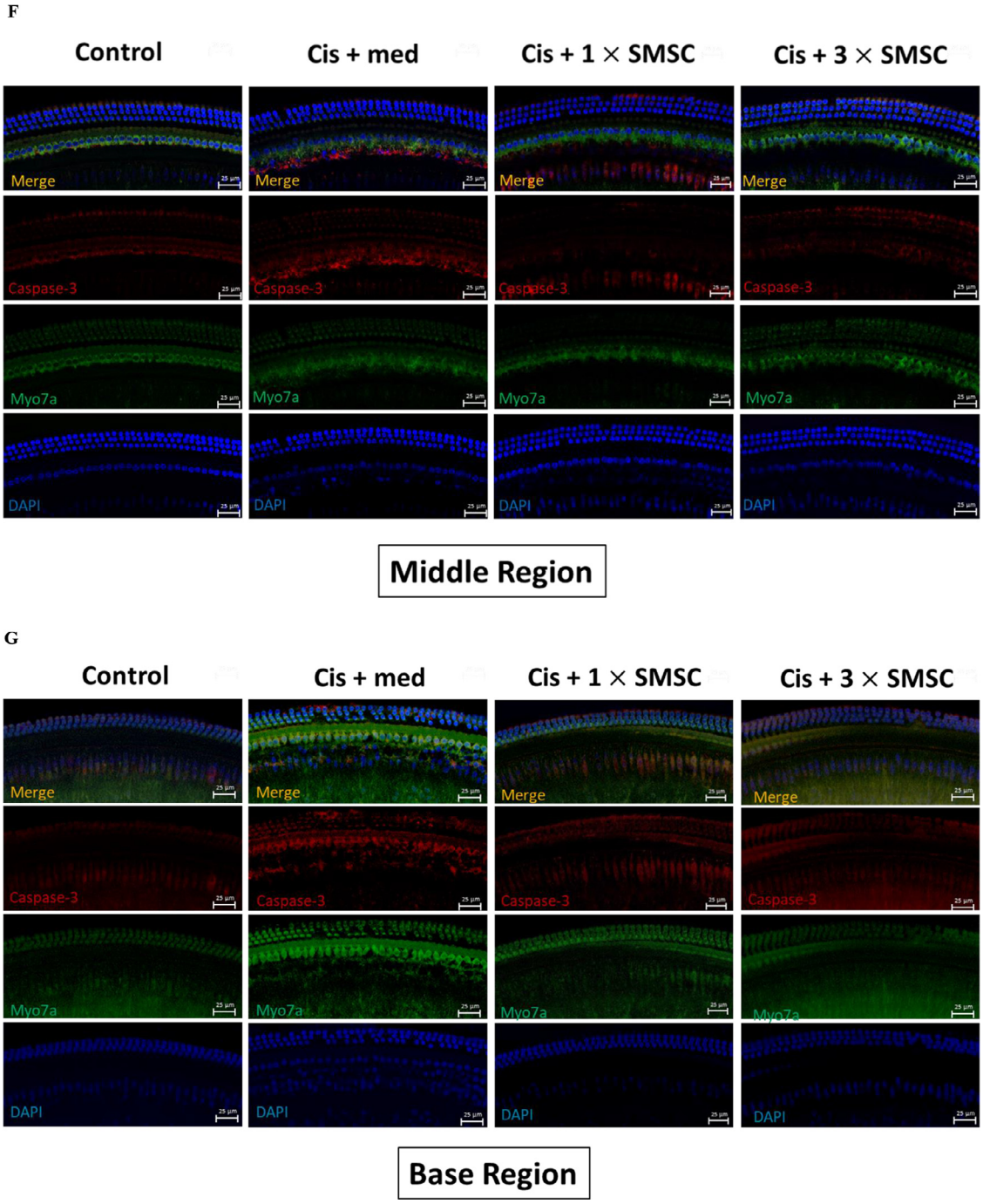

Fig. 5. Continued

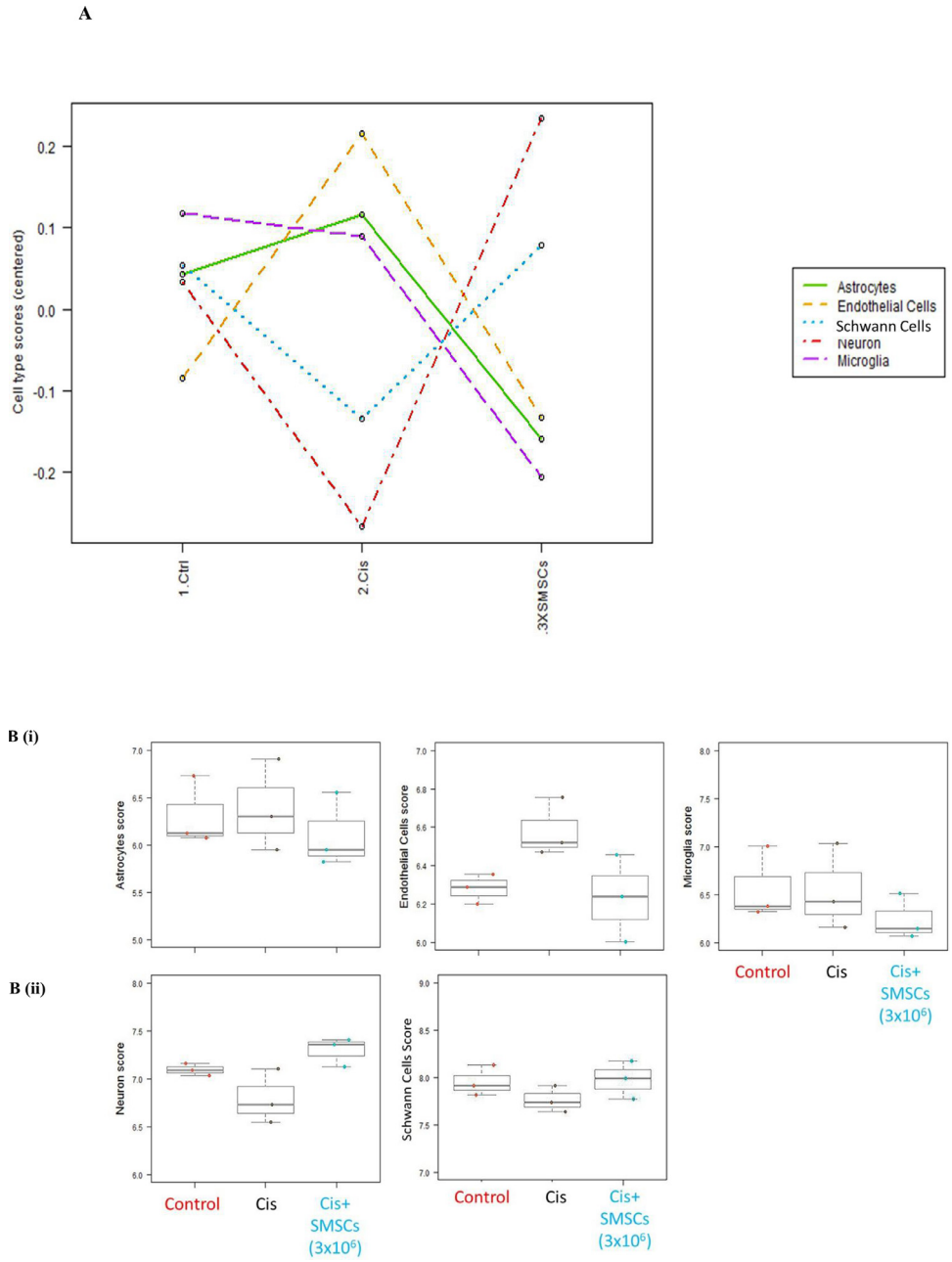

Fig. 6. Neuropathological gene panel analyses of the cell types in the cochlear tissues from mice with cisplatin-induced hearing loss. (A) Summary of the scores of cell types in the mRNA expression profiles of the cochlear tissues of three representative mice in each group. (B) Increases and decreases in the scores of cell types in the mRNA expression profiles of the cochlear tissues in three representative mice.

5. Conclusion

Although SMSCs express the NPC marker gene PAX8 (Ahn et al., 2004) (Table 3), our whole transcriptome data suggest that SMSCs and iPSC-derived NPCs have different transcriptome profile (Fig. 2 and Supplementary Fig. 1). SMSCs expressed multiple growth factors for cochlear tissue repair and exerted beneficial effects for ameliorating cisplatin-induced hearing loss in vivo. Our data suggest that SMSCs can significantly ameliorate hearing loss and decrease the loss of cochlear HCs in cisplatin-injected mice. The characteristics of SMSCs are both different and similar to those of NSPCs and OPCs. The findings of this study suggest that SMSCs can exert protective effects against ototoxic drug–induced SHL and have value for future clinical application.

Author Statement

Conceptualization: Yi-Chao Hsu.

Data curation: Stella Chin-Shaw Tsai, Frank Cheau-Feng Lin, Kuang-Hsi Chang, Min-Chih Li, Ruey-Hwang Chou, Chien-Yu Kao, Ching-Chang Cheng, Hung-Ching Lin, Yi-Chao Hsu.

Formal analysis: Min-Chih Li, Ruey-Hwang Chou, Ching-Chang Cheng, Yi-Chao Hsu.

Funding acquisition: Stella Chin-Shaw Tsai, Mei-Yue Huang, Yi-Chao Hsu.

Investigation: Stella Chin-Shaw Tsai, Frank Cheau-Feng Lin, Kuang-Hsi Chang, Min-Chih Li, Ruey-Hwang Chou, Chien-Yu Kao, Ching-Chang Cheng, Yi-Chao Hsu.

Methodology: Kuang-Hsi Chang, Min-Chih Li, Ruey-Hwang Chou, Yen-Chung Chen, Chien-Yu Kao, Ching-Chang Cheng, Hung-Ching Lin, Yi-Chao Hsu.

Project administration: Yi-Chao Hsu.

Resources: Stella Chin-Shaw Tsai, Frank Cheau-Feng Lin, Mei-Yue Huang, Yen-Chung Chen, Yi-Chao Hsu.

Supervision: Yi-Chao Hsu.

Validation: Yi-Chao Hsu.

Roles/Writing - original draft: Stella Chin-Shaw Tsai, Frank Cheau-Feng Lin, Kuang-Hsi Chang, Min-Chih Li, Ruey-Hwang Chou, Yen-Chung Chen, Chien-Yu Kao, Ching-Chang Cheng, Hung-Ching Lin, Yi-Chao Hsu.

Writing - review & editing: Stella Chin-Shaw Tsai, Frank Cheau-Feng Lin, Kuang-Hsi Chang, Min-Chih Li, Ruey-Hwang Chou, Yen-Chung Chen, Chien-Yu Kao, Ching-Chang Cheng, Yi-Chao Hsu.

Declaration of Competing Interest

Maria Von Med-Biotechnology Co., Ltd, Taiwan provided a partial grant. The authors independently characterized the SMSCs and evaluated the effects of SMSCs in cisplatin-induced hearing loss.

Stella Chin-Shaw Tsai has no relation with Maria Von Med-Biotechnology Co., Ltd.

Frank Cheau-Feng Lin has no relation with Maria Von Med-Biotechnology Co., Ltd.

Kuang-Hsi Chang has no relation with Maria Von Med- Biotechnology Co., Ltd.

Min-Chih Li has no relation with Maria Von Med- Biotechnology Co., Ltd.

Ruey-Hwang Chou has no relation with Maria Von Med-Biotechnology Co., Ltd.

Mei-Yue Huang is the founder of Maria Von Med- Biotechnology Co., Ltd.

Yen-Chung Chen was the chief technology officer in Maria Von Med- Biotechnology Co., Ltd.

Chien-Yu Kao has no relation with Maria Von Med- Biotechnology Co., Ltd.

Ching-Chang Cheng has no relation with Maria Von Med-Biotechnology Co., Ltd.

Hung-Ching Lin has no relation with Maria Von Med- Biotechnology Co., Ltd.

Yi-Chao Hsu has no relation with Maria Von Med- Biotechnology Co., Ltd.

Acknowledgment

We thank the Department of Medical Research, Tungs' Taichung Metroharbor Hospital for their grant support (TTMHH-R1100010). We thank Maria Von Med-Biotechnology Co., Ltd, Taiwan for grant support. We also thank the Ministry of Science and Technology (MOST) of the Taiwan Government for grant support (MOST 107-2314-B-715-004-MY3), and from Mackay Medical College for their intramural research grants (MMCRD-1081E03, MMCRD-1091B19). We thank Mr. Hung-Yi Tsai for his technical assistance.

Supplementary materials

Supplementary material associated with this article can be found, in the online version, at doi:10.1016/j.heares.2021.108254.

References

Ahn, J.I., Lee, K.H., Shin, D.M., Shim, J.W., Lee, J.S., Chang, S.Y., Lee, Y.S., Brownstein, M.J., Lee, S.H., Lee, Y.S., 2004. Comprehensive transcriptome analysis of differentiation of embryonic stem cells into midbrain and hindbrain neurons. Dev Biol 265, 491–501.

Akil, O., Oursler, A.E., Fan, K., Lustig, L.R., 2016. Mouse Auditory Brainstem Response Testing. Bio Protoc 6.

Aksoy, I., Giudice, V., Delahaye, E., Wianny, F., Aubry, M., Mure, M., Chen, J., Jauch, R., Bogu, G.K., Nolden, T., et al., 2014. Klf4 and Klf5 differentially inhibit mesoderm and endoderm differentiation in embryonic stem cells. Nat Commun 5, 3719.

Almeida-Branco, M.S., Cabrera, S., Lopez-Escamez, J.A., 2015. Perspectives for the treatment of sensorineural hearing loss by cellular regeneration of the inner ear. Acta Otorrinolaringol Esp 66, 286–295.

Andsberg, G., Kokaia, Z., Bjorklund, A., Lindvall, O., Martinez-Serrano, A., 1998. Amelioration of ischaemia-induced neuronal death in the rat striatum by NGF-secreting neural stem cells. Eur J Neurosci 10, 2026–2036.

Bowers, W.J., Chen, X., Guo, H., Frisina, D.R., Federoff, H.J., Frisina, R.D., 2002. Neurotrophin-3 transduction attenuates cisplatin spiral ganglion neuron ototoxicity in the cochlea. Mol Ther 6, 12–18.

Chen, Y.C., Tsai, C.L., Wei, Y.H., Wu, Y.T., Hsu, W.T., Lin, H.C., Hsu, Y.C., 2018. ATOH1/RFX1/RFX3 transcription factors facilitate the differentiation and characterisation of inner ear hair cell-like cells from patient-specific induced pluripotent stem cells harbouring A8344G mutation of mitochondrial DNA. Cell Death Dis 9, 437.

Chen, Y.S., Liu, T.C., Cheng, C.H., Yeh, T.H., Lee, S.Y., Hsu, C.J., 2003. Changes of hair cell stereocilia and threshold shift after acoustic trauma in guinea pigs: comparison between inner and outer hair cells. ORL J Otorhinolaryngol Relat Spec 65, 266–274.

Choi, M.Y., Yeo, S.W., Park, K.H., 2012. Hearing restoration in a deaf animal model with intravenous transplantation of mesenchymal stem cells derived from human umbilical cord blood. Biochem Biophys Res Commun 427, 629–636.

Fan, Z., Duan, J., Wang, L., Xiao, S., Li, L., Yan, X., Yao, W., Wu, L., Zhang, S., Zhang, Y., et al., 2019. PTK2 promotes cancer stem cell traits in hepatocellular carcinoma by activating Wnt/beta-catenin signaling. Cancer Lett 450, 132–143.

Hu, Z., Zhang, B., Luo, X., Zhang, L., Wang, J., Bojrab 2nd, D., Jiang, H., 2014. The astroglial reaction along the mouse cochlear nerve following inner ear damage. Otolaryngol Head Neck Surg 150, 121–125.

Ingham, N.J., Pearson, S., Steel, K.P., 2011. Using the Auditory Brainstem Response (ABR) to Determine Sensitivity of Hearing in Mutant Mice. Curr Protoc Mouse Biol 1, 279–287.

Jahanbazi Jahan-Abad, A., Morteza-Zadeh, P., Sahab Negah, S., Gorji, A, 2017. Curcumin attenuates harmful effects of arsenic on neural stem/progenitor cells. Avicenna J Phytomed 7, 376–388.

Jamieson, E.R., Lippard, S.J., 1999. Structure, Recognition, and Processing of Cisplatin-DNA Adducts. Chem Rev 99, 2467–2498.

Kang, E.J., Byun, J.H., Choi, Y.J., Maeng, G.H., Lee, S.L., Kang, D.H., Lee, J.S., Rho, G.J., Park, B.W., 2010. In vitro and in vivo osteogenesis of porcine skin-derived mesenchymal stem cell-like cells with a demineralized bone and fibrin glue scaffold. Tissue Eng Part A 16, 815–827.

Kasagi, H., Kuhara, T., Okada, H., Sueyoshi, N., Kurihara, H., 2013. Mesenchymal stem cell transplantation to the mouse cochlea as a treatment for childhood sensorineural hearing loss. Int J Pediatr Otorhinolaryngol 77, 936–942.

Kecskemeti, N., Gaborjan, A., Szonyi, M., Kustel, M., Baranyi, I., Molnar, M.J., Tamas, L., Gal, A., Szirmai, A., 2019. [Etiological factors of sensorineural hearing loss in children after cochlear implantation]. Orv Hetil 160, 822–828.

Kikkawa, Y.S., Nakagawa, T., Horie, R.T., Ito, J., 2009. Hydrogen protects auditory hair cells from free radicals. Neuroreport 20, 689–694.

Kil, K., Choi, M.Y., Kong, J.S., Kim, W.J., Park, K.H., 2016. Regenerative efficacy of mesenchymal stromal cells from human placenta in sensorineural hearing loss. Int J Pediatr Otorhinolaryngol 91, 72–81.

Kleiderman, S., Gutbier, S., Ugur Tufekci, K., Ortega, F., Sa, J.V., Teixeira, A.P., Brito, C., Glaab, E., Berninger, B., Alves, P.M., et al., 2016. Conversion of Nonproliferating Astrocytes into Neurogenic Neural Stem Cells: Control by FGF2 and Interferon-gamma. Stem Cells 34, 2861–2874.

Lai, D., Wang, F., Dong, Z., Zhang, Q., 2014. Skin-derived mesenchymal stem cells help restore function to ovaries in a premature ovarian failure mouse model. PLoS One 9, e98749.

Li, Q., Sun, W., Wang, X., Zhang, K., Xi, W., Gao, P., 2015a. Skin-Derived Mesenchymal Stem Cells Alleviate Atherosclerosis via Modulating Macrophage Function. Stem Cells Transl Med 4, 1294–1301.

Li, W., Wu, J., Yang, J., Sun, S., Chai, R., Chen, Z.Y., Li, H., 2015b. Notch inhibition induces mitotically generated hair cells in mammalian cochleae via activating the Wnt pathway. Proc Natl Acad Sci U S A 112, 166–171.

Li, W.W., Wei, Y.H., Li, H., Lai, D.M., Lin, T.N., 2013. Isolation and characterization of a novel strain of mesenchymal stem cells from mouse umbilical cord: potential application in cell-based therapy. PLoS One 8, e74478.

Maruyama, M., Ichisaka, T., Nakagawa, M., Yamanaka, S, 2005. Differential roles for Sox15 and Sox2 in transcriptional control in mouse embryonic stem cells. J Biol Chem 280, 24371–24379.

Meen, E., Blakley, B., Quddusi, T., 2010. Does intracochlear brain-derived nerve growth factor improve auditory brainstem click thresholds in sensorineural hearing loss? J Otolaryngol Head Neck Surg 39, 232–235.

Meng, X.M., Ren, G.L., Gao, L., Yang, Q., Li, H.D., Wu, W.F., Huang, C., Zhang, L., Lv, X.W., Li, J., 2018. NADPH oxidase 4 promotes cisplatin-induced acute kidney injury via ROS-mediated programmed cell death and inflammation. Lab Invest 98, 63–78.

Monastero, R., Garcia-Serrano, S., Lago-Sampedro, A., Rodriguez-Pacheco, F., Colomo, N., Morcillo, S., Martin-Nunez, G.M., Gomez-Zumaquero, J.M., Garcia-Fuentes, E., Soriguer, F., et al., 2017. Methylation patterns of Vegfb promoter are associated with gene and protein expression levels: the effects of dietary fatty acids. Eur J Nutr 56, 715–726.

Neal, C., Kennon-McGill, S., Freemyer, A., Shum, A., Staecker, H., Durham, D, 2015. Hair cell counts in a rat model of sound damage: Effects of tissue preparation & identification of regions of hair cell loss. Hear Res 328, 120–132.
Nicolay, N.H., Lopez Perez, R., Ruhle, A., Trinh, T., Sisombath, S., Weber, K.J., Ho, A.D., Debus, J., Saffrich, R., Huber, P.E., 2016. Mesenchymal stem cells maintain their defining stem cell characteristics after treatment with cisplatin. Sci Rep 6, 20035.
Ninoyu, Y., Sakaguchi, H., Lin, C., Suzuki, T., Hirano, S., Hisa, Y., Saito, N., Ueyama, T., 2020. The integrity of cochlear hair cells is established and maintained through the localization of Dia1 at apical junctional complexes and stereocilia. Cell Death Dis 11, 536.
Noda, M., Hatano, M., Hattori, T., Takarada-Iemata, M., Shinozaki, T., Sugimoto, H., Ito, M., Yoshizaki, T., Hori, O., 2019. Microglial activation in the cochlear nucleus after early hearing loss in rats. Auris Nasus Larynx 46, 716–723.
Nold, P., Hartmann, R., Feliu, N., Kantner, K., Gamal, M., Pelaz, B., Huhn, J., Sun, X., Jungebluth, P., Del Pino, P., et al., 2019. Correction to: Optimizing conditions for labeling of mesenchymal stromal cells (MSCs) with gold nanoparticles: a prerequisite for in vivo tracking of MSCs. J Nanobiotechnology 17, 98.
Park, B.W., Kang, D.H., Kang, E.J., Byun, J.H., Lee, J.S., Maeng, G.H., Rho, G.J., 2012. Peripheral nerve regeneration using autologous porcine skin-derived mesenchymal stem cells. J Tissue Eng Regen Med 6, 113–124.
Ringborg, U., 1983. [The importance of controlling the side effects of antineoplastic therapy with cisplatin]. Lakartidningen 80, 2240–2241.
Rubino, S.J., Mayo, L., Wimmer, I., Siedler, V., Brunner, F., Hametner, S., Madi, A., Lanser, A., Moreira, T., Donnelly, D., et al., 2018. Acute microglia ablation induces neurodegeneration in the somatosensory system. Nat Commun 9, 4578.
Shi, F., Kempfle, J.S., Edge, A.S., 2012. Wnt-responsive Lgr5-expressing stem cells are hair cell progenitors in the cochlea. J Neurosci 32, 9639–9648.
Singh, S.P., Tripathy, N.K., Nityanand, S., 2013. Comparison of phenotypic markers and neural differentiation potential of multipotent adult progenitor cells and mesenchymal stem cells. World J Stem Cells 5, 53–60.
Spangenberg, E., Severson, P.L., Hohsfield, L.A., Crapser, J., Zhang, J., Burton, E.A., Zhang, Y., Spevak, W., Lin, J., Phan, N.Y., et al., 2019. Sustained microglial depletion with CSF1R inhibitor impairs parenchymal plaque development in an Alzheimer's disease model. Nat Commun 10, 3758.
Sun, Y., Jin, K., Childs, J.T., Xie, L., Mao, X.O., Greenberg, D.A., 2006. Vascular endothelial growth factor-B (VEGFB) stimulates neurogenesis: evidence from knockout mice and growth factor administration. Dev Biol 289, 329–335.
Toma, J.G., Akhavan, M., Fernandes, K.J., Barnabe-Heider, F., Sadikot, A., Kaplan, D.R., Miller, F.D., 2001. Isolation of multipotent adult stem cells from the dermis of mammalian skin. Nat Cell Biol 3, 778–784.
Toma, J.G., McKenzie, I.A., Bagli, D., Miller, F.D., 2005. Isolation and characterization of multipotent skin-derived precursors from human skin. Stem Cells 23, 727–737.
Tomfohr, J., Lu, J., Kepler, T.B., 2005. Pathway level analysis of gene expression using singular value decomposition. BMC Bioinformatics 6, 225.
Uutela, M., Lauren, J., Bergsten, E., Li, X., Horelli-Kuitunen, N., Eriksson, U., Alitalo, K, 2001. Chromosomal location, exon structure, and vascular expression patterns of the human PDGFC and PDGFD genes. Circulation 103, 2242–2247.
Veceric-Haler, Z., Cerar, A., Perse, M., 2017. (Mesenchymal) Stem Cell-Based Therapy in Cisplatin-Induced Acute Kidney Injury Animal Model: Risk of Immunogenicity and Tumorigenicity. Stem Cells Int 2017, 7304643.
Vemaraju, S., Kantarci, H., Padanad, M.S., Riley, B.B., 2012. A spatial and temporal gradient of Fgf differentially regulates distinct stages of neural development in the zebrafish inner ear. PLoS Genet 8, e1003068.
Wang, Q., Chen, R., Zhang, C., Inam, U.L., Piao, F., Shi, X., 2019. NGF protects bone marrow mesenchymal stem cells against 2,5-hexanedione-induced apoptosis in vitro via Akt/Bad signal pathway. Mol Cell Biochem 457, 133–143.
Wang, S.F., Chen, M.S., Chou, Y.C., Ueng, Y.F., Yin, P.H., Yeh, T.S., Lee, H.C., 2016. Mitochondrial dysfunction enhances cisplatin resistance in human gastric cancer cells via the ROS-activated GCN2-eIF2alpha-ATF4-xCT pathway. Oncotarget 7, 74132–74151.
Wu, X., Li, X., Song, Y., Li, H., Bai, X., Liu, W., Han, Y., Xu, L., Li, J., Zhang, D., et al., 2017. Allicin protects auditory hair cells and spiral ganglion neurons from cisplatin - Induced apoptosis. Neuropharmacology 116, 429–440.
Yang, D., Zhou, H., Zhang, J., Liu, L., 2015. Increased endothelial progenitor cell circulation and VEGF production in a rat model of noise-induced hearing loss. Acta Otolaryngol 135, 622–628.
Yang, Q., Sun, G., Yin, H., Li, H., Cao, Z., Wang, J., Zhou, M., Wang, H., Li, J., 2018. PINK1 Protects Auditory Hair Cells and Spiral Ganglion Neurons from Cisplatin-induced Ototoxicity via Inducing Autophagy and Inhibiting JNK Signaling Pathway. Free Radic Biol Med 120, 342–355.
Yang, Y., Liu, S., Gao, H., Wang, P., Zhang, Y., Zhang, A., Jia, Z., Huang, S., 2020. Ursodeoxycholic acid protects against cisplatin-induced acute kidney injury and mitochondrial dysfunction through acting on ALDH1L2. Free Radic Biol Med 152, 821–837.
Zhang, Y., Chen, Y., Li, B., Ding, P., Jin, D., Hou, S., Cai, X., Sheng, X., 2020. The effect of monotropein on alleviating cisplatin-induced acute kidney injury by inhibiting oxidative damage, inflammation and apoptosis. Biomed Pharmacother 129, 110408.
Zhou, J., An, C., Jin, X., Hu, Z., Safirstein, R.L., Wang, Y, 2020. TAK1 deficiency attenuates cisplatin-induced acute kidney injury. Am J Physiol Renal Physiol 318, F209–F215.